SHRINKAGE INDUCED DEFORMATIONS

IN COMPOSITE STEEL AND

CONCRETE BRIDGES

By
IBRAHIM SABRI ABDELMEGUID
Bachelor of Science in Civil Engineering
Cairo University
Giza, Egypt
2011

Submitted to the Faculty of the
Graduate College of the
Oklahoma State University
in partial fulfillment of
the requirements for
the Degree of
MASTER OF SCIENCE
May, 2015

SHRINKAGE INDUCED DEFORMATIONS

IN COMPOSITE STEEL AND

CONCRETE BRIDGES

Thesis Approved:

Bruce W. Russell

Thesis Adviser

Tyler Ley

Julie Hartell

DEDICATION

I dedicate my work to my loving parents, Sabri and Einas for the unconditional love and support they gave me. My brothers who have never left my side, especially my twin Mohamed. My nephews for all lovely time I spent with them, especially Tarek. I dedicate this work to all my friends for their words of encouragement and special thanks to Hesham Allam and Bassam Amr.

Acknowledgements reflect the views of the author and are not endorsed by committee members or Oklahoma State University.

ACKNOWLEDGEMENTS

The author would like to acknowledge the Oklahoma department of transportation for funding this research work. I am indebted to my advisor and committee chair, Dr. Bruce Russell, for all his time and support. I wish to thank my committee members, Dr. Tyler Ley and Dr. Julie Hartell, for all their time and effort. Special thanks to Dr. Robert Emerson for his warm welcome to Oklahoma state University. I acknowledge OSU for furnishing me with this opportunity to pursue my graduate degree, which allowed me to grow personally and professionally.

Name: IBRAHIM ABDELMEGUID

Date of Degree: MAY, 2015

Title of Study: SHRINKAGE INDUCED DEFORMATIONS IN COMPOSITE STEEL AND CONCRETE BRIDGES

Major Field: CIVIL ENGINEERING

Abstract: Concrete decks cast on steel bridge girders experience volume change beginning immediately after taking initial set. Volume changes in concrete result from temperature changes, creep or drying shrinkage of concrete. Shrinkage of the concrete occurs from a combination of hydration and evaporation as water is either consumed or pulled from the concrete. Resulting volume changes are the usual sources for cracking in concrete, serviceability problems and excessive deflections in deck slabs, sidewalks, driveways and other pavements, however they do not cause structural collapse alone. A poor prediction of such volumetric changes can be regarded as unimportant but it is important for some structures where serviceability and economic feasibility are needed. Recently, some Oklahoma bridges have been rehabilitated by casting new concrete decks atop existing steel girders. Some of these bridges experienced excessive downward deflections soon after construction was completed. Our research shows that concrete strains caused by drying shrinkage may account for some of these mid-span deflections.

In our research, prototype beams were constructed from steel girders made composite with concrete deck slabs. These beams were monitored for temperature, concrete and steel strains and deflections. Results of the prototypes show downward deflections and concrete compressive strains consistent with the phenomenon of concrete shrinkage. Test results are compared to analytical iterative models that focus on concrete shrinkage. Models are based on ACI 209R-92 report shows methods for predicting creep, shrinkage and temperature effects in concrete structures. Three other numerical methods are compared in these reports and include the Bazant-Baweja B3 model, the CEB MC90-99 model and the GL2000 model. The four models are compared to one another and with the experimental results from the prototype beam constructed in lab. Some concrete properties were tested in the laboratory to use in the models. Despite the laboratory findings which connect concrete shrinkage to downward deflections of steel girder bridges, forensic investigations performed on real highway bridges that show the bridges were in a good condition and that shrinkage is not the likely cause of excessive deflections.

TABLE OF CONTENTS

LIST OF TABLES

LIST OF FIGURES

CHAPTER I

INTRODUCTION

1.1 Background

Concrete bridge decks cast atop steel bridge girders experience volume changes beginning immediately after taking initial set. Volume changes in concrete can result from temperature changes, creep and drying shrinkage of concrete. Shrinkage of the concrete occurs from the combination of hydration and evaporation as water is either consumed by hydration or pulled from the concrete by evaporation. Resulting volume changes are the usual causes for cracking in concrete. Rarely do volume changes in concrete cause structural failures. A poor prediction of such volumetric changes can be important for some structures where serviceability is an important criterion.

Recently some Oklahoma bridges have been rehabilitated by casting new concrete deck slabs atop of existing steel girders. Some of these bridges experienced excessive downwards deflections at mid-spans soon after construction were completed making those bridges have bad ride quality. Our research shows that concrete strains caused by drying shrinkage may account for some of these mid-span deflections.

1.2 Scope

In our research, prototype beams were constructed from steel girders made composite with concrete deck slabs. These beams were monitored for temperature, concrete strains and deflections. Results of the prototypes show downward deflections and concrete compressive strains consistent with the phenomenon of concrete shrinkage. Test results are compared to analytical iterative models that focus on concrete shrinkage and temperature variations. Models are based on ACI reports 209.2R-08 and 209R-92, the 209.2R-08 reports shows methods of predicting creep, shrinkage and temperature effects in concrete structures, also four numerical models are compared in these reports used. Models used are from ACI 209R-92, Bazant-Baweja B3 model, CEB MC90-99 model and GL2000 model, the four models are compared to each other and with the data collected from the prototype beam constructed in lab.

Unrestrained shrinkage specimens were also cast to measure unrestrained shrinkage. Concrete cylinders and other samples were collected to quantify and establish material properties for the concrete.

1.3 Research Objectives

- Determine the effects of shrinkage and other time dependant properties of concrete decks on the deflection of steel girders.
- Assess whether time dependent properties of shrinkage or creep or other volumetric changes in concrete represent possible causes for unwanted deflections in bridges.

CHAPTER II

BACKGROUND AND LITERATURE REVIEW

2.1 Background

Three bridges were identified in 2012 in Woods Co. Oklahoma as possessing poor ride quality. It was suggested by some that excessive deflections in steel composite bridges are caused by the phenomenon of concrete shrinkage. In composite construction, new concrete decks are poured atop and made composite with existing steel girders. As the concrete cures and ages, it shrinks.

Shrinkage is a regular and well recognized property of concrete. Concrete shrinkage is caused by a combination of evaporation of free water and the use of pore water in hydration of cement after concrete has taken initial set. Both evaporation and the use of water in hydration cause negative pressures in the pore structures of hardened concrete. This in turn causes the concrete to shrink.

It has been theorized that concrete shrinkage causes the deck slab to shorten, and the deck's shortening causes composite steel girder bridges to deflect downward.

Bridges around the state have been identified around the State of Oklahoma that may be affected by this phenomenon. In addition to the three bridges in Woods Co., one in Payne Co. and one near Eufaula have also been identified.

2.2 Different Approaches to Predict Shrinkage Effects

Some information regarding the effects of slab shrinkage on bridge deck deflection exists in the literature, but the mechanics can also be derived theoretically. Composite bridges are constructed by placing slab concrete on steel girders or precast prestressed girders with shear connectors to guarantee monolithic behavior (Tonias, 1995). A good assessment of shrinkage and creep effects on the stress and deflection responses of a structure is important to meet the ultimate and serviceability limit states required by different codes (Amadio & Fragiacomo, 1997).

Different approaches for evaluating and predicting creep and shrinkage effects in different structures are discussed in this chapter as well as explaining those effects on composite concrete-steel beams.

One simplified approach to evaluate creep and shrinkage effects in steel-concrete composite beams with rigid and deformable connections has been introduced by (Amadio & Fragiacomo, 1997) based on what they called age-adjusted effective modulus method. The authors introduced an aging coefficient "x" to the popular effective modulus method and found out that their method can substitute the latter for considering time-dependent long term effects. The authors believe that the use of stronger design materials in recent history has led to an increase in extreme fibers strains at service loads. As a result, deflection limits may govern the design of composite beams more and more.

In their paper the authors characterized three algebraic methods, namely the effective modulus (EM) method, the mean stress (MS) method and the age-adjusted effective

modulus (AAEM) method in case an accurate evaluation of time dependent effects is required. The value "x" was calculated one time for creep in a concrete beam under sustained load and another time in a shrinkage problem. The authors found out that the usage of their approach permits a simple solution of viscous problems in steel-concrete composite beams with rigid or deformable connections when concrete is considered un-cracked. Comparing the solutions obtained using this approach to the ones obtained by the EM and MS methods showed the advantage of this approach specifically for shrinkage problems. The authors also recommended to use the EM method if the effects of viscous problems are not important.

Birkeland presented an analytical method to predict the downward deflections which occurs in beams due to shrinkage stresses in concrete deck slab (Birkeland, 1960). Birkeland believes that shrinkage in a slab cast onto precast prestressed beams induces stress into the composite beams. He attributed the shrinkage to normal aging and curing processes. The author gave equations for stresses on slab and beam section, slope and deflection. This was followed by a comparison of computed values with actual values obtained from full size test beams. It is believed that the given approach, with reasonable assumptions, can be used for other several cases of composite beams like the case of steel-concrete composite beams. Values were found to be close. In their method, an approach that obtains shrinkage by means of self-cancelling externally applied forces is used; this method was employed by (Ferguson, 1958).

The author also acknowledged the time dependent changes in Young modulus; however he used a constant value for the modulus to limit the number of time-

dependent factors. For simplicity Birkeland considered only simple spans, constant area properties throughout the length of the beam and elastic behavior (un-cracked concrete where plane sections remain plane).

Birkeland concluded that it is possible to predict deflections caused by shrinkage in composite beams. However some experience in choosing values of Young modulus and shrinkage may be needed as those two factors are highly affected by the quality and quantity of the concrete mixture and the quality control procedures when the concrete is placed and cured.

Birkeland concluded that it is possible to predict deflections caused by shrinkage in composite beams. However some experience in choosing values of Young modulus and shrinkage may be needed as those two factors are highly affected by the quality and quantity of the concrete mixture and the quality control procedures when the concrete is placed and cured. Birkeland also recommends applying the method presented in their paper on similar problems, concrete-steel combination with a model to determine strain and stresses in overlaid beams was developed by (Silfwerbrand, 1997). The model is based on a linear relationship between slip and shear stress at the interface, the model dealt with full slip, partial bond and complete bond. Uniform shrinkage distribution in the slab (overlay) was assumed although the maximum shrinkage usually occurs at top surface, a full contact between the slab and beam was assumed- which means the curvature of the slab and overlaid beam will be the same- also in addition to Bernoulli's hypothesis, that the plane sections remain plane after bending, differential shrinkage tests on two concrete beams have been carried out, the author found out that the restrained shrinkage cannot be computed by multiplying the

measured strain and the modulus of elasticity, also they found that the concrete creep has a big influence on shrinkage stresses, since a part of the shrinkage stresses is released due to increasing creep.

Another new proposed method for monitoring early age shrinkage known as the layer approach starting 30 minutes after water is added to the mixture was introduced by (Kwak, Seo, & Jung, 2000), in the article the authors studied the shrinkage effect of concrete by the volume change of concrete slabs, to verify analytical results, field tests were performed on two bridges under construction. Shrinkage strain was evaluated directly using shrinkage models found in design codes (ACI Committee 3. , 1989) and is defined as the volume change that occurs independently of imposed stresses (Kwak, Seo, & Jung, 2000). After obtaining the strains, stresses were calculated using the constitutive model. The neutral axis was located in a time step fashion. The neutral axis location was found to change due to the changes in the elastic modulus of the concrete slab with time. Then the internal forces and unbalanced forces were calculated. Based on their findings, shrinkage strains monitored through image analysis or the layer approach compared well with the experimental results. Also, the field conditions were found to affect the ultimate shrinkage strain, so effective quality control for deck concrete was found to be important. Finally no visible transverse cracks at the interior supports of tested bridges were found.

Prediction equations and empirical equations proposed by many researchers like the ones proposed by (Bazant & Panula, 1978), by Branson (ACI, Prediction of creep, shrinkage and temperature effects in concrete structures, 1982) and others are

practical and useful for the preliminary study at the design stage (Eguchi & Teranishi, 2005), however the accuracy of these predicted models are not very good and even reported to be around plus or minus 40% (Japan, 2001), reasons behind this were considered to be that most of the prediction equations are empirical equations derived from the measured data which involves some errors during statistical studies, also the effects of the material properties are hard to obtain. For that, Eguchi in their study tried to develop a complex model to a practical prediction equation taking into account the internal factors of concrete while keeping the temperature and humidity and member shape and size constant. For developing such equation the author measured the independent factors of the prediction equation and verified their complex model to experimental results for concrete samples, finally in this study a prediction equation of drying shrinkage for concrete at any age based on complex model was proposed and its applicability was tested, accuracy was found to be minimal. However the values for Young modulus estimated by this method were found to be less than real values.

2.3 Effect of Concrete Shrinkage on Composite Steel Beams

"Concrete shrinks. Not much, but enough to warrant thinking about in design. Steel Doesn't, so in composite construction shrinkage of in-situ concrete slabs induces stresses And deflections in the supporting steel beams" (Alexander, 2003).

Alexander in his paper (Alexander, 2003) says that shrinkage can be important for two aspects of serviceability, stress limitation and deflection. The author explained the theory of shrinkage and how to calculate the effects. Numerical examples were

used. For simplicity Alexander limited his article to simply supported beams in indoor conditions.

Alexander first derived what he called the “contraction force” in the slab and then characterized the sources of this contraction into early thermal and shrinkage contractions. Early thermal contraction is caused when the fresh concrete cools down and hardens after being heated by the exothermal chemical reaction of hydration. However since the heat of hydration in the case of composite slabs can escape from the top and bottom surfaces of concrete, the author decided to ignore the early thermal contraction. Instead the author determined that shrinkage is more important, most especially the drying shrinkage. The author applied the contraction force he derived “F” as an external force to the steel beam (not the composite section), then he applied basic mechanics of materials to compute stresses in extreme fibers; compression in the top and tension in the bottom. He also calculated curvature and deflection, curvature was calculated using the M/EI formula and deflection as 0.125*k (L) 2, where k is the curvature and L is the span of a simple supported beam. The author found out that it is acceptable to ignore the tensile stresses in the bottom fiber of the steel girder induced by shrinkage since the service loads are usually over-estimated and the design stress is less than the yield stress. However for deflection calculations, Alexander recommends including the shrinkage deflection as part of the total long term deflection. The author also suggests that “L/750” as a simple rule for designers to account for shrinkage deflection can be assumed unless a more accurate calculation is used, this deflection limit is a conservative one based on his calculations on beams with different depths.

Figure 1 Time Dependent Deflections on Girder FZ2450-3 (Russell 1992) and Figure 2 Time Dependent Deflections DZ2450-1 (Russell 1992) (Russell B. W., 1992) show the deflection vs. time for a beam before and after concrete pouring for a composite concrete-prestressed beam.

The graphs show the downward deflections that took place after the concrete was cast caused by the weight of fresh concrete, and then an upward deflection of the composite beam in response of heating of the slab caused by concrete hydration after the initial set had taken place. As the slab cools and the concrete shrinks, a downward deflection takes place. This response is very typical for composite beams.

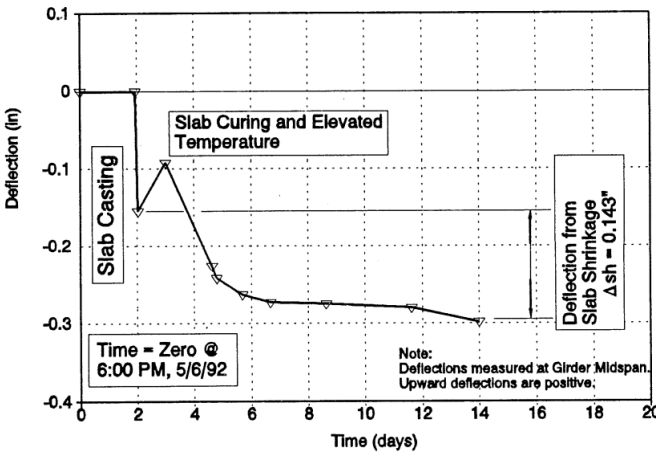

FIgure 7.42 Time Dependent Deflections: DZ2450-1

Figure 1 Time Dependent Deflections on Girder FZ2450-3 (Russell 1992)

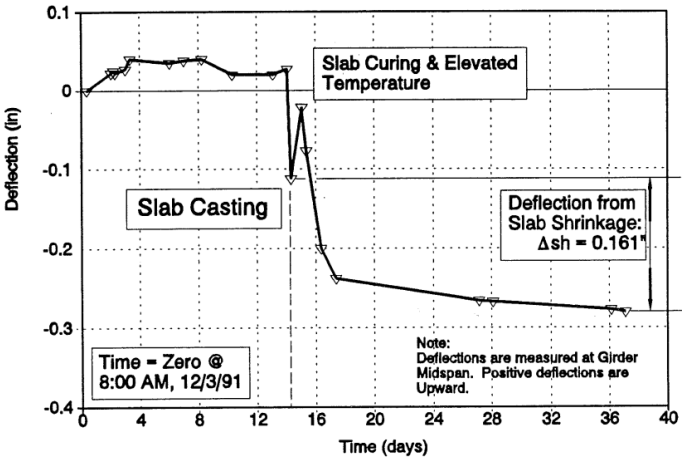

FIgure 7.41 Time Dependent Deflections: FZ2450-3

Figure 2 Time Dependent Deflections DZ2450-1 (Russell 1992)

Figure 3 Residual Strains and Positive Curvature resulting from Slab Shrinkage shows a schematic for the basic mechanism of how shrinkage strains in the concrete deck slab can cause bending strains in the precast concrete beam cross section. As mentioned before the shrinkage force at the centroid of the deck slab is considered an external force on the beam. The external force here – considered being the shrinkage force- is equilibrated by a curvature in the precast concrete beam.

Theoretically, the curvature of the cross section will be uniform all along the span length, and the resulting deflection can be related directly to cross section curvature as shown in Figure 4 Deflection caused by slab shrinkage (Russell 1992)

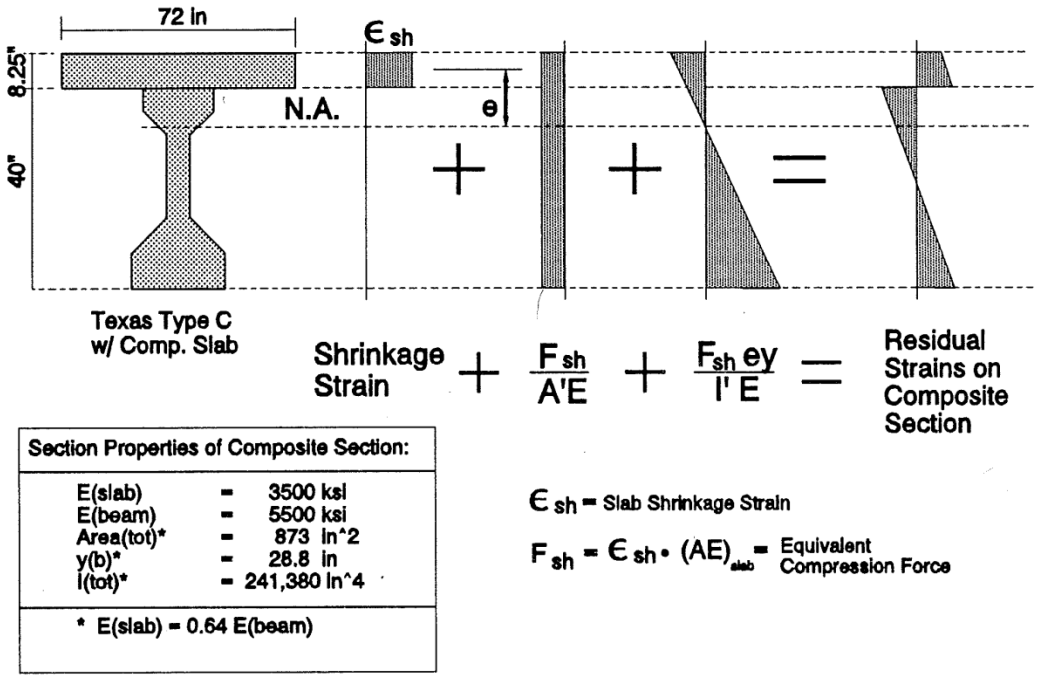

Figure 7.44 Residual Strains from Slab Shrinkage

Figure 3 Residual Strains and Positive Curvature resulting from Slab Shrinkage (Russell 1992)

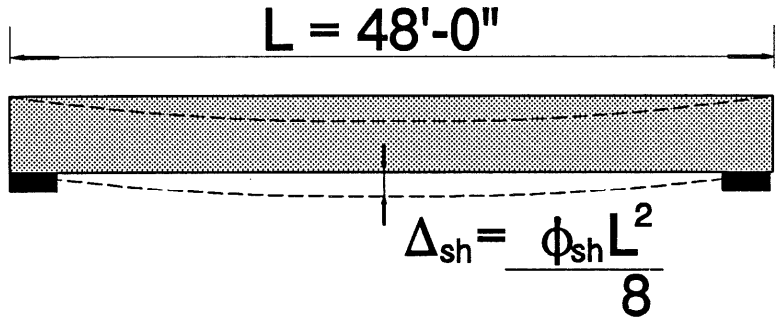

Figure 7.43 Deflection from Shrinkage

Figure 4 Deflection caused by slab shrinkage (Russell 1992)

In the computations performed by Russell, a short term elastic modulus was used since the age of the slab concrete was relatively young at the time deflections were

measured. When considering the long term effects from these phenomena, one would more correctly employ an effective *modulus* which could account for the effect of creep in concrete as time goes by (Russell B. a., 1993).

2.4 Popular Numerical Models for Predicting Shrinkage Models

Numerical models were built and used to estimate concrete shrinkage strains and beam deflections; from those we can develop an idea of internal stresses developed, and estimate whether cracking will occur in the deck slabs. Four models, valid for hardened concrete that is moist cured for at least one day, are used and compared to one another and to the results obtained from the prototype beams.

All of the models made assumptions on behavior and material properties. Here are some of the assumptions that were common: (ACI, Guide for Modeling and Calculating Shrinkage and Creep in Hardened Concrete, 2008)

- Shrinkage and creep are independent of each other.
- Shrinkage is divided into autogenous shrinkage and drying shrinkage.
- Differential shrinkage and creep or shrinkage and creep gradients are neglected.

Also definitions were set in the same report (ACI, Guide for Modeling and Calculating Shrinkage and Creep in Hardened Concrete, 2008):

Autogenous shrinkage: The shrinkage occurring in the absence of moisture exchange (as in sealed concrete specimen) due to the hydration reactions taking place in the cement matrix. Also called basic/chemical shrinkage.

Drying shrinkage: Shrinkage occurring in a specimen allowed to dry.

Shrinkage: The strain measure in a load-free concrete specimen.

Primary concrete characteristics needed for the prediction models were found to be:

- Mix proportions
- Compressive and tensile strength and elasticity.
- Ambient relative humidity
- Duration of drying
- Specimen size (volume to surface ratio)

Models used can substitute different value of elastic modulus which is a major time dependent factor, also are easy to use and not so sensitive to all input parameters.

2.4.1.1 ACI 209R-92 Model

The model recommended by ACI Committee (ACI, "Prediction of Creep, Shrinkage, and Temperature Effects in Concrete Structures (ACI 209R-92)", 1992) was developed by (Branson & Christiason, 1971) .According to the ACI 209.2R-08 Report it is easy to use with minimal background knowledge. Also, it is easy to fit short term data by changing the ultimate shrinkage value. Also the model is empirically based. Basic requirements for using the model will be the drying time, curing method, cement type, volume to surface ratio and the relative humidity.

In the following equation given in ACI 209 (1992), the shrinkage strain is a function of the age of the concrete it days, t, the age of the concrete when moist curing was removed, t_c, and parameters f (days) and α based on the member shape and size that define the time-ratio part. A is taken equal to 1 for flatter hyperbolic form. Also, one must assume

or measure the ultimate shrinkage value, epsilon shu. The shrinkage strain $\varepsilon_{sh}(t,t_c)$ at age of concrete t (days), measured from the start of drying at t_c (days), is calculated by the following equation:

$$\varepsilon_{sh}(t,t_c) = \frac{(t-t_c)^{\alpha}}{f+(t-t_c)^{\alpha}} \cdot \varepsilon_{shu}$$

ε_{shu} is the ultimate shrinkage strain and an average suggested value of 780×10^{-6} in/in. is used.

For standard conditions a relative humidity of 40% is assumed.

Where f is recommended to be 35 for 7 days of moist curing and α is suggested to be taken as 1.0, for other conditions than the standard f is given as:

$$f = 26.0e^{\{0.36\left(\frac{V}{S}\right)\}}$$

The value f is taken in the model as 35 but is corrected to account for 1 day moist curing instead of 7 days.

Where (V/S) is the volume to surface ratio in inches.

For conditions different than the standard conditions, the ultimate shrinkage ε_{shu} is modified by seven factors accounting for different curing times, relative humidity, size of member, slump factor, aggregate and cement contents.

The cumulative product of all applicable correction factors is called γ_{sh} and is multiplied by ε_{shu} to give a better estimate for the ultimate shrinkage strain.

The following table shows the different inputted values used in the model.

Considered corrections were taken to account for the following:

- V/S ratio.
- Aggregate factor, using the aggregate content in the mix design.
- Cement content factor
- Air content factor
- Slump of fresh concrete factor.
- Ambient relative humidity factor.
- Moist curing factor.

2.4.1.2 Bažant-Baweja B3

B3 model (Bažant & Baweja, 1995,2000) is the second model used in this thesis to predict shrinkage strains, and according to the ACI 209.2R-08 Report it is useful for simple and complex structures, also the model separates basic and drying creep. Basic requirements for using the model will be the drying time, curing method, cement type, cement content, concrete mean compressive strength at 28 days, water content in concrete, volume to surface ratio and the relative humidity.

The time function was given as follows:

$$\varepsilon_{sh}(t,t_c) = -\varepsilon_{sh\infty} k_h S(t-t_c)$$

Where $\varepsilon s_{h\infty}$ is the ultimate shrinkage strain, k_h is the humidity dependence factor, $S(t-t_c)$ is the time curve, and $(t-t_c)$ is the time from the end of initial curing.

The ultimate shrinkage strain is given by the equation:

$$\varepsilon_{sh\infty} = -\varepsilon_{s\infty} \frac{E_{cm607}}{E_{cm(t_c+\tau_{sh})}}$$

Where $\varepsilon_{s\infty}$ is a constant function of concrete unit weight and the 28 days compressive strength, and $E_{cm607}/E_{cm}(t_c+ \tau_{sh})$is a factor to account for the time dependence of ultimate shrinkage.

$$\varepsilon_{s\infty} = -\alpha_1\alpha_2\{0.02565w^{2.1}f_{cm28}{}^{-0.28} + 270\]x\ 10^{-6}$$

Where w is the water content in lb/yd^3, f_{cm28} is the concrete mean compressive strength at 28 days in psi, α_1 and α_2 are constant to account for the cement type and curing condition.

$$E_{cmt} = E_{cm28}(\frac{t}{(4+0.85t)})^{0.5}$$

Where E_{cm28} is the mean modulus of elasticity of concrete at 28 days in psi.

The time function for shrinkage $S(t-t_c)$ is given by:

$$S(t-t_c) = tanh\sqrt{\frac{(t-t_c)}{\tau_{sh}}}$$

Where t and t_c are the age of concrete and the age when moist curing ends in days, respectively.

$\boldsymbol{\tau}_{sh}$ is the shrinkage half-time in days, given by:

$$\tau_{sh} = 0.085t_c{}^{-0.08}\, f_{cm28}{}^{-0.25}\left\{2k_s(\frac{V}{S})\right]^2$$

Where Ks is the cross section shape-correction factor, and V/S is the volume to surface ratio in inches.

This method also gives a time dependent value for the elastic modulus E_{cmt} which was used for the rest of the three models also for further accuracy.

The following tables show the inputted date for both prototype beams # 1 and # 2 respectively.

2.4.1.3 CEB MC90-99 Model

CEB Model Code 1990-99 (Muller & Hilsdorf, 1990), (CEB, "Evaluation of The Time Dependent Properties of Concrete,", 1991) (CEB, "CEB-FIP Model Code 1990,", 1993) (CEB, "Structural Concrete—Textbook on Behaviour, Design and Performance. Updated Knowledge of the CEB/FIP Model Code 1990,", 1993) (CEB, "Structural Concrete—Textbook on Behaviour, Design and Performance. Updated Knowledge of the CEB/FIP Model Code 1990,", 1999) for prediction of shrinkage and creep in concrete is the third model used in this research, the model was revised in 1999 (béton, 1999) to include high strength concrete and also to separate the shrinkage into autogenous and drying shrinkage, and it is called CEB MC90-99 Model.

The total shrinkage strains of concrete $\varepsilon sh(t,t_c)$ is given by the following equation:

$$\varepsilon_{sh}(t, t_c) = \varepsilon_{cs0}\beta_s(t - t_c)$$

Where ε_{cso} is the notional shrinkage coefficient, $\beta_s(t - t_c)$ is the coefficient describing the development of shrinkage with time of drying, t is the age of concrete (days) and t_c is the day of the end of moist curing.

The notional shrinkage coefficient is given by:

$$\varepsilon_{cs0} = \varepsilon_s f_{cm28}\beta_{RH}(h)$$

with

$$\varepsilon_s(f_{cm28}) = 160 + 10\beta_{sc}\left(9 - \frac{f_{cm28}}{f_{cm0}}\right)x10^{-6}$$

$$\beta_{RH}(h) = -1.55\left[1 - \left(\frac{h}{h_0}\right)^3\right] \text{ for } 0.4 < h < 0.99$$

$$\beta_{RH}(h) = 0.25 \text{ for } h > 0.99$$

Where f_{cm28} is the mean compressive strength of concrete of 28 days in psi, f_{cm0} is equal to 1450 psi, β_{sc} is a coefficient that depends on the type of cement, h is the ambient relative humidity as a decimal and h_0 equal to 1.

The shrinkage development with time is given by:

$$\beta_s(t - t_c) = \left[\frac{(t - t_c)/t_1}{350\left[\left.V/S\right/V/S_0\right]^2 + (t - t_c)/t_1}\right]^{0.5}$$

Where $(t\text{-}t_c)$ is the duration of drying in days, t_1 is equal to 1 day, V/S is the volume to surface ratio in inches and $(V/S)_0$ is equal to 2 in.

The actual duration of drying can be used although the method assumes curing period of 14 days at least, but this duration does not affect the shrinkage significantly.

This model splits the total shrinkage into autogenous and drying shrinkage, the autogenous shrinkage component is given by:

$$\varepsilon_{cas}(t) = \varepsilon_{cas0} f_{cm28} \beta_{as}(t)$$

Where ε_{cas0} is the notional autogenous shrinkage coefficient and β_{as} is the time development function of the autogenous shrinkage.

$$\varepsilon_{cas0}(f_{cm28}) = -\alpha_{as}[\frac{(f_{cm28}/f_{cm0})}{6 + (f_{cm28}/f_{cm0})}]^{2.5} \text{ x } 10^{-6}$$

$$\beta_{as}(t) = 1 - \exp[-0.2(\frac{t}{t_1})^{0.5}]$$

Where f_{cm28} is the mean compressive strength of concrete at the age of 28 days in psi, f_{cm0} = 1450 psi, t is the concrete age (days), t_1 = 1 day and α_{as} is a coefficient accounting for the type of cement.

The drying shrinkage is given by the following equation:

$$\varepsilon_{cds0}(f_{cm28}) = [(220 + 110\alpha_{ds1})\exp(-\alpha_{ds2}f_{cm28}/f_{cm0})]\text{x } 10^{-6}$$

$$\beta_{RH}(h) = -1.55[1 - (\frac{h}{h_0})^3] \text{for } 0.4 < h < 0.99\beta_{s1}$$

$$\beta_{RH}(h)0.25 \text{ for } h > 0.99\beta_{s1}$$

$$\beta_{ds}(t - t_c) = [\frac{(t - t_c)/t_1}{350[{}^{V}\!/_{S}\,/\,{}^{V}\!/_{S_0}]^2 + (t - t_c)/t_1}]^{0.5}$$

$$\beta_{s1} = [\frac{(3.5f_{cm0})}{f_{cm28}}]^{0.1} < 1$$

Where α_{ds1} and α_{ds2} are coefficients that depend on the type of cement, β_{s1}takes self desiccation in high performance concrete, h is the ambient relative humidity as a decimal as h_0 = 1, V/S is the volume to surface ratio, $(V/S)_0$ = 2in., f_{cmo} = 1450 psi, t_c is the age of concrete at the end of moist curing (days), and $(t-t_c)$ is the drying time (days).

According to the ACI 209.2R-08 Report the model is preferred for shrinkage sensitive structures.

Basic requirements for using the model will be the drying time, curing method, cement type, concrete mean compressive strength at 28 days, volume to surface ratio and the relative humidity.

2.4.1.4 GL2000 Model

The GL model developed by (Gardner & Lockman, 2001) and made to conform to the ACI model guidelines.

The model requires age of concrete when drying starts, cement type, volume to surface ratio and concrete mean compressive strength at 28 days.

$$\varepsilon_{sh}(t, t_c) = \varepsilon_{shu}\beta(h)\beta(t - t_c)$$

Where ε_{shu} is the ultimate shrinkage strain, $\beta(h)$ is the correction factor for the effect of humidity and $\beta(t\text{-}t_c)$ is a correction term for the effect of time drying.

$$\varepsilon_{shu} = 900k\left(\frac{4350}{f_{cm28}}\right)^{0.5} x\ 10^{-6}$$

Where fcm28 is the concrete mean compressive strength at 28 days in psi and k is shrinkage constant depending on cement type.

$$\beta(h) = (1 - 1.18h^4)$$

Where h is the humidity as a decimal.

$$\beta(t - t_c) = \left[\frac{(t - t_c)}{(t - t_c) + 77(V/S)^2}\right]^{0.5}$$

Where t and t_c are the age of concrete and the age of end of moist curing in days, respectively, and V/S is the volume-surface ratio in inches

CHAPTER III

STUDY METHEDOLOGY

3.1 Concrete Properties

Concrete conforming the ODOT AA specifications was made in the laboratory and material properties of those concrete mixtures were tested. Tests were conducted to determine the fresh and hardened concrete properties. Fresh properties included concrete slump, unit weight, air content, concrete temperature and ambient temperature. Hardened properties included concrete compressive strength, elastic modulus and splitting tensile strength. A summary of those tests is discussed. Table 1 shows the mixture proportions for the ODOT AA concrete.

Table 1 Batch weight/Volume and SSD weights

AA Batch Weight/Volume and SSD Weights				
Water to Cement	0.44			
Cement	611	lb/y^3	3.11	ft^3
Fly Ash	0	lb/y^3	0	ft^3
Coarse	1900	lb/y^3	11.28	ft^3
Fine	1217	lb/y^3	7.36	ft^3
Water	269	lb/y^3	4.31	ft^3
Air			0.94	ft^3
			27	ft^3

Figure 5 shows a concrete cylinder after having a compressive strength test ASTM C39 applied on it, figure shows a typical cone failure. Figure 6 shows a cylinder set up to have the elastic modulus test ASTM C469., Figure 7 shows a typical splitting cylinder tensile testing failure done in the laboratory, while Figure 8 shows the setup for the splitting cylinder tensile strength test ASTM C496 test.

All of the laboratory material characterization tests were conducted on ODOT AA concrete mixture described in Table 1 above. The ODOT AA concrete mixture was specified for both Prototype Beam #1 and Prototype Beam #2. Concrete for the two prototypes was ordered and delivered from a local ready mix concrete producers. For the mixture, cast upon Prototype Beam #1, the concrete mixture exhibited a slump of about 4.5 in. when discharged from the truck. Though this was workable concrete, the slump

loss was noticeable and significant as concrete was placed in cylinders, in the shrinkage prisms and in deck of Prototype Beam #1. We note that the mixture contained a mid-range water reducer.

For Prototype Beam #2, cast a few days after Prototype Beam #1, in initial slump was again measured at about 3 to 4 in. So for this batch, water was added to the concrete while still on the ready mix truck until the initial slump was increased to 9 in. We note that for both days of casting the prototype beams, the concrete temperatures exceeding 90 F, and the slump loss that was exhibited is consistent with the elevated concrete temperature. Both mixtures contained a mid-range water reducer.

In addressing the added water, the batch size for each concrete truck was a total of about 2.0 CY of concrete. For the second concrete batch, on Prototype Beam #2 we added approximately 10 gallons of water – which is 83 lbs. If we consider that water addition, the w/cm for the second batch of concrete is reduced from 0.44 to 0.50. However, we strongly suspect that the ready mix company withheld water from both batches though we do not have any direct evidence. Regardless, the empirical information suggests that the mixture for Prototype Beam # 2 had about a 0.06 w/cm higher than that for Prototype Beam # 1.

Figure 5 Type 1 failure (cone failure)

Figure 6 Set up of the elastic modulus test

Figure 7 Split tensile failure

Figure 8 The setup of the splitting tensile strength test

3.2 Prototype Beams

Two prototype beams were built where steel girders were made composite with concrete deck slabs. W8x15 sections were chosen with a center to center span of 12 feet.

3.2.1.1 Design of Prototype Beams

Two Prototype beams were designed for an average tensile stress in the concrete slab to resemble the average tensile stress in the real concrete deck of the bridge passing through the SH 86, having 8 inches slab cast on W33x141 girder.

An ultimate design shrinkage of 500 microstrains is assumed since shrinkage is not yet known and is assumed to be restrained. This restrained shrinkage can be converted to a theoretical restraining force by multiplying it by the concrete modulus of elasticity. The tensile restraining force will act in the centroid of the concrete slab whick will be equilibrated by an eccentric compressive force applied on the composite section.

The eccentric compressive force will induce axial stress (P/A) and bending stress (My/I) into the composite section.

The shrinkage strain in the concrete slab being restrained due to the composite action taking place after the bridge being rehabilitated will cause a resultant force in the centroid of the slab having an arm to the neutral axis of the composite section to cause curvature in the beam which results in some deflection taking place.

This theoretical method also assumed the 28 days concrete compressive strength to be 4000 psi, and the concrete modulus of elasticity to be 57000√f'c, which gave 3605 ksi.

A perfect bond between layers is assumed to ensure composite action.

3.2.1.2 Analysis of SH86 Bridge

The SH86 was chosen to be analyzed since it had the worst ride quality out of the three bridges investigated. Figure 9 shows the theoretical method used to analyze the bridge. Cross section properties are shown for the bridge girder W33x141 having a slab of 8 in. thick atop of it. Composite section properties are calculated.

The average tensile stress in the concrete deck was 364 psi. The prototype beam was designed to give a similar or close average tensile stress in its concrete deck using the same assumptions and the same theoretical method.

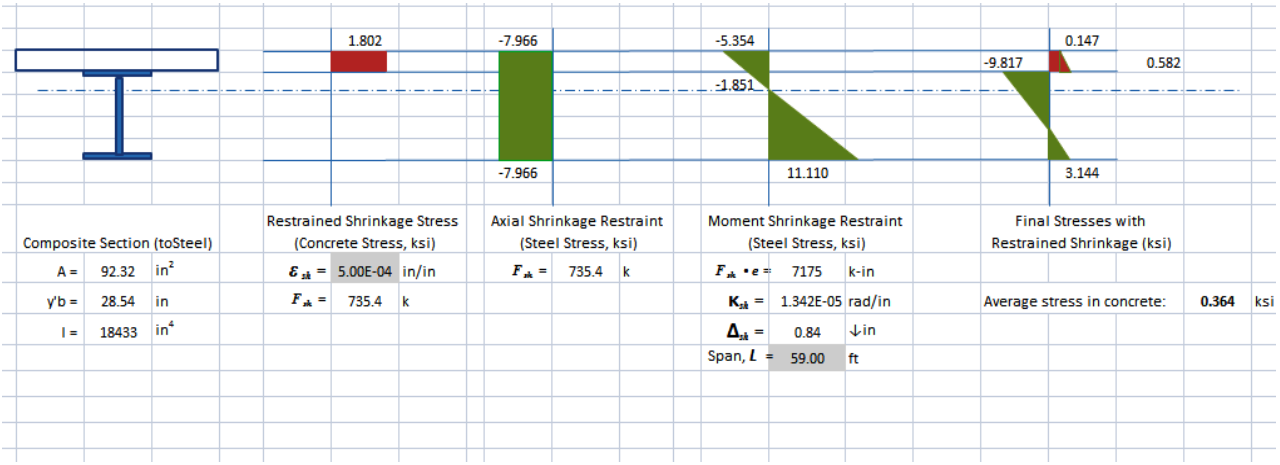

Figure 9: Stresses due to restrained shrinkage in concrete deck slab of SH86 Bridge over Stillwater Creek in Payne Co.

3.2.1.3 Design of Prototype Beam# 1

Figure 10 shows the analysis of prototype beam # 1 to give a close average tensile stress in the deck slab, using W8x15 and 3 in. deck slab cast a top of it gave an average tensile stress of 341 psi which is very close to the one in SH86, given the same assumptions.

The figure shows the resulting axial and bending stresses on the composite cross section.

Figure 10: Stresses due to restrained shrinkage in concrete deck slab of Prototype beam #1 proportioned to resemble the SH86 Bridge

3.2.1.4 Design of Prototype Beam# 2

Another prototype beam# 2 is made with 4.5 inches slab instead of 3 inches; it also had different concrete mix design in order to consider the effect of different water content.

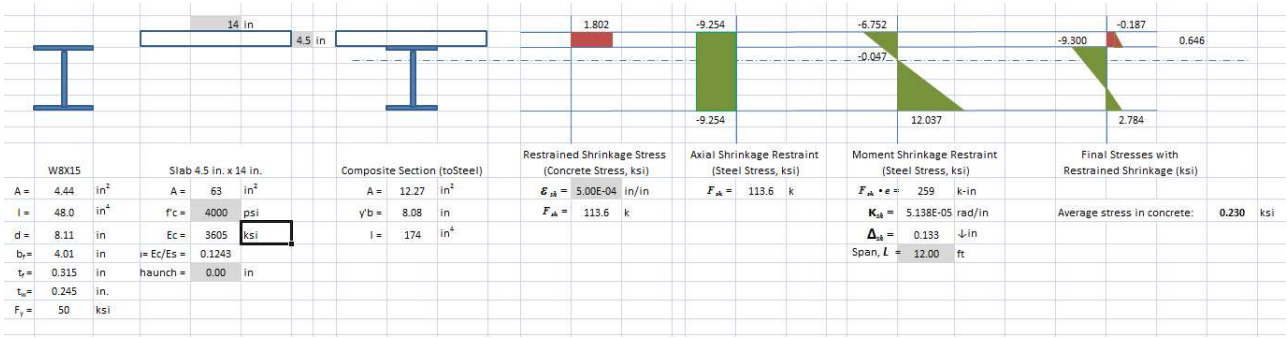

Figure 11 Stresses due to restrained shrinkage in concrete deck slab of Prototype beam #2 proportioned to resemble the SH86 Bridge

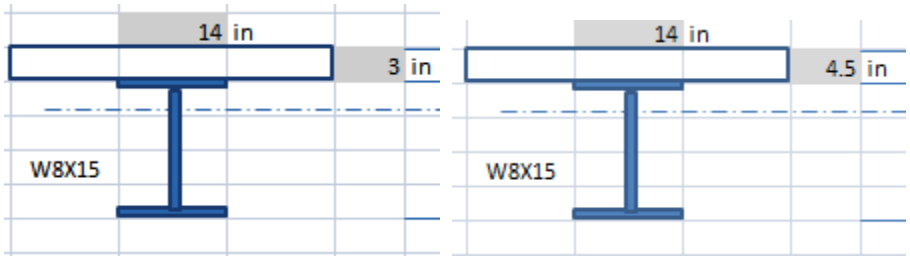

Figure 12 Shows cross-sections for prototype beams 1 & 2

3.2.1.5 Shrinkage prisms

Shrinkage prisms were cast from the ready mix concrete that was used to cast the composite slab atop the Prototype Beams, direct shrinkage measurements were done on them to get the unrestrained strains and compare it later on to the restrained concrete strains at the top of concrete slab.

3.2.1.6 Data collected from the Prototype beams

Thermocouples embedded in the concrete were used to measure the temperature gradient, also strain measuring device was employed to measure steel and concrete strains, mechanical strain gage (DEMEC gage) was the one used. Using the strain readings together with the temperature gradient will enable us to study the contribution that concrete shrinkage has on deflection of the composite beam. Deflection gage is also used to measure the deflection at midspan of the beam over time. Deck slabs of the beams were made of ODOT AA concrete mixtures used in the original bridge decks.

The following figures illustrate the measurements taken from the composite beams, figure 13 shows the deflection gage being setup at the midspan of the beam, zero reading was taken to illuminate the deflection due to the self-weight of the cast slab.

Figure 14 shows the thermocouples used to develop the temperature gradient while figure 15 shows the thermocouples getting embedded in the cast slab.

Figure 16 shows the deflection gage at the midspan and also shows the DEMEC points glued on the top surface of the concrete slab. A thermometer was also embedded in the concrete slab to be able to take immediate readings for concrete and steel temperatures as shown in figure 17.

Figure 13 Deflection gage set up at the midspan of the beam.

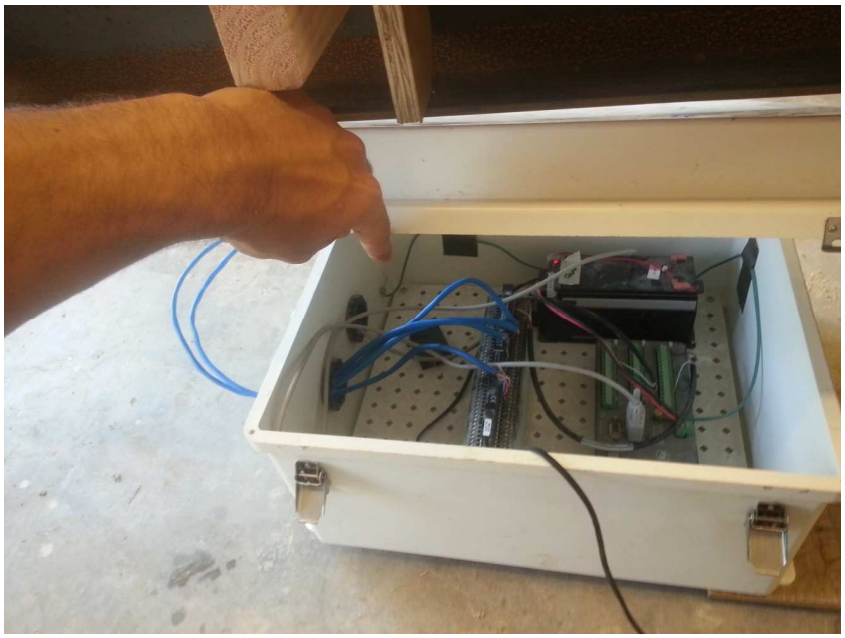

Figure 14 Thermocouples used to develop temperature gradient

Figure 15 Thermocouples embedded in concrete deck slab

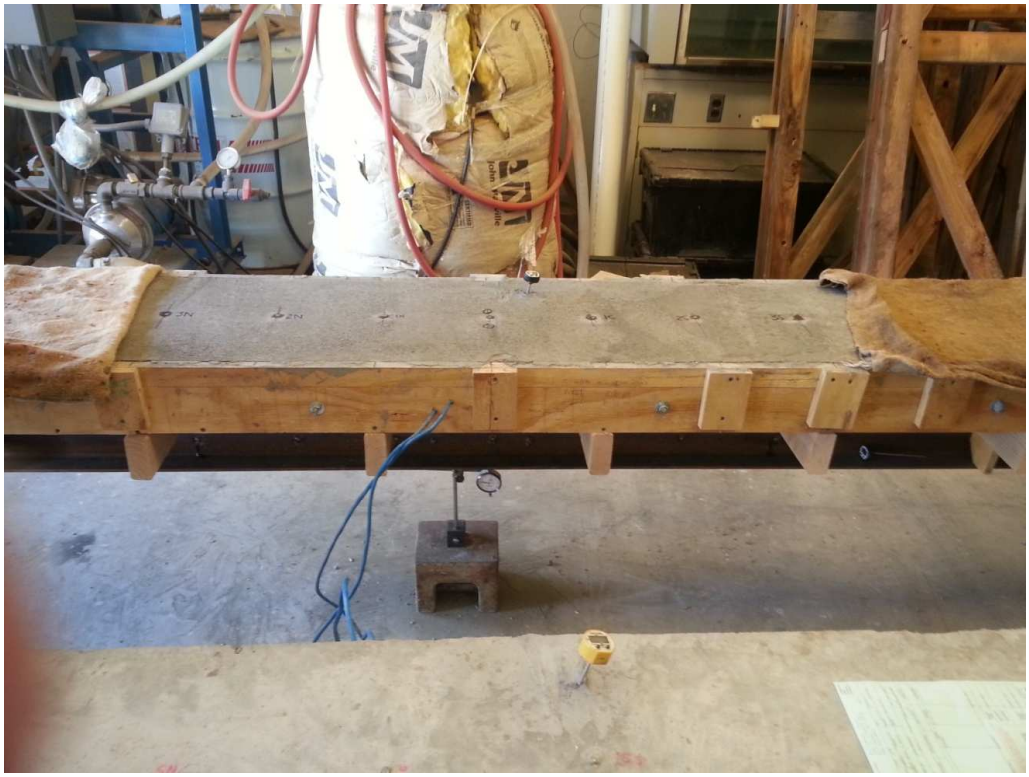

Figure 16 Deflection gage at mid-span to measure deflection

Figure 17 Thermometers were also embedded in concrete to take immediate readings

Figure 14 shows the prototype beam#1 with the 3 in. deck slab cast atop of the steel girder while prototype beam# 2 with the 4.5 in. slab is ready to get the concrete placed.

Figure 18 Prototype beam # 1 is cast and beam # 2 is ready to get concrete placed.

Moist curing was done for one day as shown in figure 15.

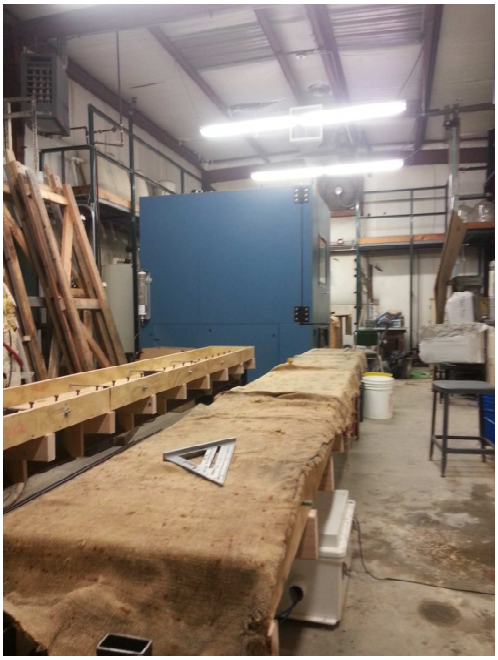

Figure 19 Concrete slabs were moist cured for one day

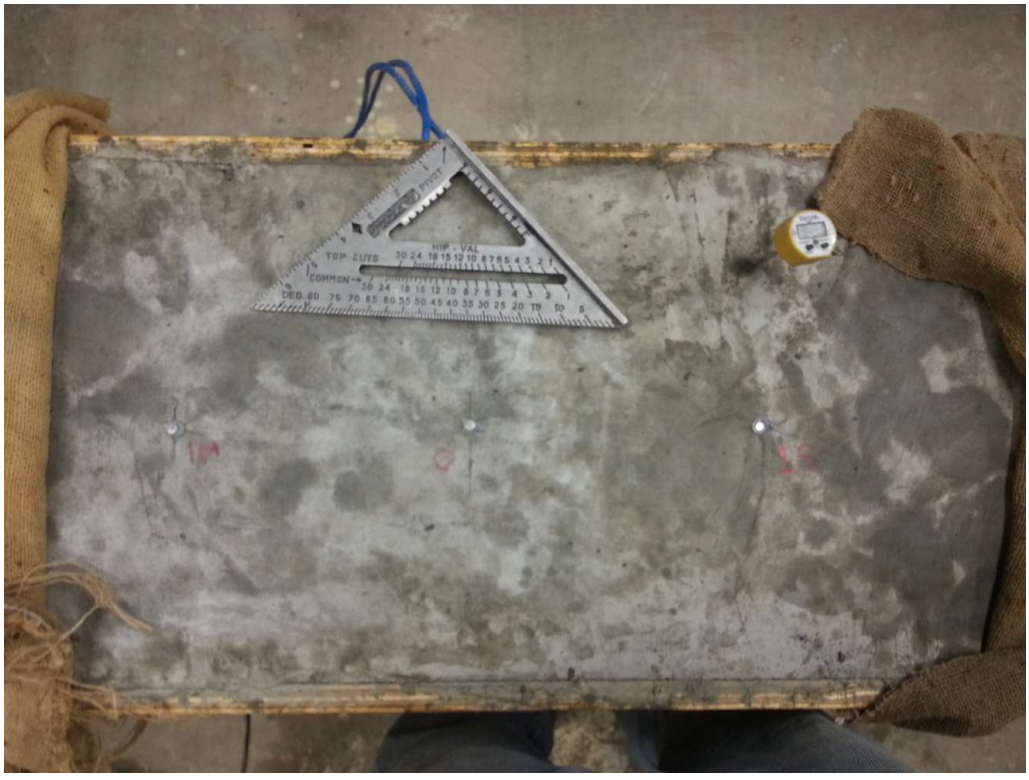

Figure 20 DEMEC points were glued to take strain readings out of them later on

Figure 20 **DEMEC points were glued to take strain readings out of them later on** shows DEMEC points glued to the surface of concrete slab, they were also glued to certain locations of the steel beam to measure:

- Concrete surface strains (DEMEC) at top surface of the slabs.
- Steel surface strains on the steel beam web at 1.75 in from the bottom flange of beam 1 and 2 in. from the bottom flange of beam 2.
- Unrestrained shrinkage on beam specimens.
- Beam deflections
- Cracks were being observed visually.

Figure 21 Shows DEMEC points glued on the surface of the web at 1.75 inches from the bottom flange of prototype beam A

Figure 22 Shows gages for measuring changes in beams deflection at mid-span. The gages are accurate to 0.001 in.

3.3 Numerical Models for Predicting Shrinkage

Popular models shown in the literature review are used to predict shrinkage strains, and using the same theoretical method discussed in section.

Table 2 tabulates general inputted date for the four models used; the data includes values for the concrete compressive strength obtained from lab experimentation, ambient relative humidity, ambient temperature, volume to surface ratio and curing time and condition for prototype beam # 1.

While table 3 shows mix proportions and fresh and hardened concrete properties for prototype beam# 1.

Same Inputted data for prototype beam # 2 is shown in table 4.

Table 2 Shows inputted problem data for prototype beam # 1

Problem Data:		
Concrete Data:		
Specified 28-day strength	f'c (psi)=	6510
Ambient conditions:		
Relative humidity	h =	0.4
Temperature	T (˚F)	68
Specimen:		
Volume-surface ratio	V/S (in.) =	0.75
Shape	Infinite slab	
Initial curing:		
Curing time	t_c (days) =	1
Curing condition:	1	
Concrete at loading:		
Age at loading:	t_0(days) =	14
Applied stress range	k_s (%) =	40

Table 3 Shows mix proportions and fresh concrete properties for prototype beam #1

Estimated concrete properties:		
Mean 28-day strength	f_{cm28} (psi) =	6510
Mean 28-day elastic modulus	E_{cm28} (psi) =	6,444,000
Concrete mixture:		
Cement type:		1
Maximum aggregate size (in.)		0.75
Cement contrnt	c (lb/yd^3) =	611
Water content	w (lb/yd^3) =	268.84
Coarse aggregate (lb/yd^3) =		1900
Fine aggregate (lb/yd^3) =		1217
Water cement ratio	w/c =	0.44
Agregate cement ratio:	a/c =	5.10
Fine aggregate percentage	Ψ (%) =	39.04
Air content	α (%) =	2.7
Slump	s (in.) =	4.5
Unit weight of concrete	γ_c (lb/yd^3) =	4177
	γ_c (lb/ft^3) =	154.64

Table 4 Problem data, estimated concrete properties, mix proportions and fresh concrete properties for prototype beam #2

Problem Data:		
Concrete Data:		
Specified 28-day strength	f'c (psi)=	5340
Ambient conditions:		
Relative humidity	h =	0.4
Temperature	T (˚F)	68
Specimen:		
Volume-surface ratio	V/S (in.) =	1
Shape	Infinite slab	
Initial curing:		
Curing time	t_c (days) =	1
Curing condition:	1	
Concrete at loading:		
Age at loading:	t_0(days) =	14
Applied stress range	k_s (%) =	40

Estimated concrete properties:		
Mean 28-day strength	f_{cm28} (psi)	5340
Mean 28-day elastic modulus	E_{cm28} (psi)	5276000

Concrete mixture:		
Cement type:		1
Maximum aggregate size (in.)		0.75
Cement contrnt	c (lb/yd^3) =	611
Water content	w (lb/yd^3) =	268.84
Coarse aggregate (lb/yd^3) =		1900
Fine aggregate (lb/yd^3) =		1217
Water cement ratio	w/c =	0.44
Agregate cement ratio:	a/c =	5.10
Fine aggregate percentage	Ψ (%) =	39.04
Air content	α (%) =	4
Slump	s (in.) =	9
Unit weight of concrete	γ_c (lb/yd^3) =	4105
	γ_c (lb/ft^3) =	152

3.3.1.1 ACI 209R-92 Model

The ACI model shown in the literature review is used. Table 4 shows the correction factors to modify the 780 microstrains ultimate shrinkage recommended by the model.

Seven correction factors are applied to account for different conditions other than the standard conditions and in order to use the 780 microstrains.

The cumulative product of the seven factors is given as follows:

$\gamma_{sh} = \gamma_{sh,tc}\gamma_{sh,RH}\gamma_{sh,vs}\gamma_{sh,s}\gamma_{sh,\psi}\gamma_{sh,c}\gamma_{sh,\alpha}$

$\gamma_{sh,tc}$ is the initial moist curing factor and is given as 1.2 for 1 day moist curing.

$\gamma_{sh,RH}$ is the ambient relative humidity factor and is given as:

$\gamma_{sh,\,RH} =$

$1.40 - 1.02h$ for $0.40 \leq h \leq 0.80$

3.00 $3.0h$ for $0.80\ h < 1$; where h is the relative humidity in decimals.

The $\gamma_{sh,vs}$ is the factor that accounts for the volume surface ratio

$\gamma_{sh,\,vs} = 1.2e^{\{-0.12(V/S)\}}$

$\gamma_{sh,d}$ accounts for the thickness of the member $\gamma sh,\ d = 1.23 - 0.038d$, *where d is the thickness in inches.*

For concrete composition, factors for slump, cement content and air content are also used and shown in the following tables.

Table 6 shows the correction factors for beam # 1 while Table 5 shows the correction factors for beam # 2.

Table 5 Shows shrinkage time function used in ACI 209R-92 model, correction factors to assumed ultimate shrinkage of 780 micro-strains are also shown, values are for prototype beam # 1

ACI Model Shrinkage strains		$\varepsilon_{sh}(t,t_c)$
Nominal ultimate shrinkage strain (in./in		0.00078
Correction factors:		
Moist curing correction factor	$\gamma_{sh,tc}$ = 1.202-0.2337log(t	
	$\gamma_{sh,tc}$ =	**1.202**
Ambient relative humidity factor	γ_{RH} = 1.4-1.02*h if 0.4< h<	
	$\gamma_{sh,RH}$ = 3-3*h if 0.8< h< 1	
	$\gamma_{sh,RH}$ =	**0.992**
V/S ratio factor	$\gamma_{sh,vs} = 1.2e^{[-0.12(V/S)]}$	
	$\gamma_{sh,vs}$ =	**1.097**
Slump of fresh concrete factor	$\gamma_{sh,s}$ = 0.89+0.041s	
	$\gamma_{sh,s}$ =	**1.075**
Fine aggregate factor	γ_{ψ} = 0.30 + 0.014Ψ if Ψ <	
	γ_{ψ} = 0.90 + 0.002Ψ if Ψ >	
	$\gamma_{sh,\psi}$ =	**0.847**
Cement content factor	$\gamma_{sh,c}$ = 0.75 + 0.00036c	
	$\gamma_{sh,c}$ =	**0.970**
Air content factor	$\gamma_{sh,\alpha}$ = 0.95 + 0.008α > 1	
	$\gamma_{sh,\alpha}$ =	**1.00**
Comulative correction factor	$\gamma_{h,tc}\gamma_{sh,RH}\gamma_{sh,vs}\gamma_{sh,s}\gamma_{sh,\psi}\gamma$	
	γ_{sh} =	**1.154**
Ultimate shrinkage strain	$\gamma_{shu} = 780\gamma_{sh} \times 10^{-6}$	
	γ_{shu} =	0.00090
Shrinkage time funtion:	$(t,t_c) = [(t-t_c)^{\alpha}/(f+(t-t_c)^{\alpha}$	
Shrinkage strains:	$t,t_c) = [(t-t_c)^{\alpha}/(f+(t-t_c)^{\alpha})]$	
α = 1	f (days) = 35	

Table 6 Shows shrinkage time function used in ACI 209R-92 model, correction factors to assumed ultimate shrinkage of 780 micro-strains are also shown, values are for prototype beam # 2

Shrinkage strains	$\varepsilon_{sh}(t,t_c)$		
Nominal ultimate shrinkage strain (in./in			0.00078
Correction factors:			
Moist curing correction factor		$_{h,tc}$ = 1.202-0.2337log(	
		$\gamma_{sh,tc}$ =	**1.202**
Ambient relative humidity factor		= 1.4-1.02*h if 0.4< h	
		$_{sh,RH}$ = 3-3*h if 0.8< h<	
		$\gamma_{sh,RH}$ =	**0.992**
V/S ratio factor		$\gamma_{sh,vs} = 1.2e^{[-0.12(V/S)]}$	
		$\gamma_{sh,vs}$ =	**1.064**
Slump of fresh concrete factor		$\gamma_{sh,s}$ = 0.89+0.041s	
		$\gamma_{sh,s}$ =	**1.259**
Fine aggregate factor		= 0.30 + 0.014Ψ if Ψ <	
		= 0.90 + 0.002Ψ if Ψ >	
		$\gamma_{sh,\Psi}$ =	**0.847**
Cement content factor		$\gamma_{sh,c}$ = 0.75 + 0.00036c	
		$\gamma_{sh,c}$ =	**0.970**
Air content factor		$_{sh,\alpha}$ = 0.95 + 0.008α >	
		$\gamma_{sh,\alpha}$ =	**1.00**
Comulative correction factor		$_{tc}\gamma_{sh,RH}\gamma_{sh,vs}\gamma_{sh,s}\gamma_{sh,\Psi}$	
		γ_{sh} =	**1.312**
Ultimate shrinkage strain		$\gamma_{shu} = 780\gamma_{sh} \times 10^{-6}$	
		γ_{shu} =	0.00102
Shrinkage time funtion:		$_{,t_c}) = [(t-t_c)^{\alpha}/(f+(t-t_c)$	
Shrinkage strains:		$_{t_c}) = [(t-t_c)^{\alpha}/(f+(t-t_c)^{\alpha}$	
α =	1	f (days) =	35

3.3.1.2 Bažant-Baweja B3

B3 model presented in the literature review is used.

The time function was given as follows:

$$\varepsilon_{sh}(t,t_c) = -\varepsilon_{sh\infty}k_h S(t-t_c)$$

Where $\varepsilon s_{h\infty}$ is the ultimate shrinkage strain, k_h is the humidity dependence factor, $S(t-t_c)$ is the time curve, and $(t-t_c)$ is the time from the end of initial curing.

Tables 7 and 8 show the correction values used for beams # 1 and # 2 respectively.

The factors included cement type, curing condition and member shape factors. This resulted in an ultimate design shrinkage strain of 570 microstrains.

Table 7 Shows shrinkage time function used in B3 model, correction factors are also shown, values are for prototype beam # 1

Shrinkage strains $\varepsilon_{sh}(t,t_c)$		
Ambient relative humidity factor	$k_h = -0.2$ if $h = 1$	
	$k_h = 12.74 - 12.94h$ if $0.98 < h < 1$	
	$k_h = 1 - h^3$ if $h < 0.98$	
	$k_h =$	0.936
Nominal ultimate shrinkage	$\varepsilon_{s\infty} = -\alpha_1\alpha_2[0.02565w^{2.1}f_{cm28}^{-0.28} + 270] \times 10^{-6}$	
	$\varepsilon_{s\infty} =$	-5.47E-04
Correction factors:		
Cement type factor	$\alpha_1 =$	1
Curing condition factor	$\alpha_1 =$	1
Member shape factor	ks =	1
Shrinkage half time	$\tau_s = 190.8t_c^{-0.08}f_{cm28}^{-0.25}[2k_s(V/S)]^2$	
	$\tau_{sh} =$	47.793
Time dependence factor	$E_{cm607}/E_{cm(tc+\tau sh)} = 1.0805/[(t_c+\tau_{sh})/(4 + 0.85\,(t_c+\tau_{sh}))]^{0.5}$	
	$E_{cm607}/E_{cm(tc+\tau sh)} =$	1.043
Ultimate shrinkage strain	$\varepsilon_{sh\infty} = -\varepsilon_{s\infty}(E_{cm607}/E_{cm(tc+\tau sh)})$	
	$\varepsilon_{sh\infty} =$	-5.71E-04
Shrinkage time function	$S(t-t_c) = \tanh[(t-t_c)/\tau_{sh}]^{0.5}$	
Shrinkage strains	$\varepsilon_{sh}(t-t_c) = -\varepsilon_{sh\infty}k_h\tanh[(t-t_c)/\tau_{sh}]^{0.5}$	

Table 8 Shows shrinkage time function used in B3 model, correction factors are also shown, values are for prototype beam # 2

Shrinkage strains $\varepsilon_{sh}(t,t_c)$		
Ambient relative humidity factor	$k_h = -0.2$ if $h = 1$	
	$k_h = 12.74 - 12.94h$ if $0.98 < h < 1$	
	$k_h = 1 - h^3$ if $h < 0.98$	
	$k_h =$	0.936
Nominal ultimate shrinkage	$\varepsilon_{s\infty} = -\alpha_1\alpha_2[0.02565w^{2.1}f_{cm28}^{-0.28} + 270] \times 10^{-6}$	
	$\varepsilon_{s\infty} =$	-5.63E-04
Correction factors:		
Cement type factor	$\alpha_1 =$	1
Curing condition factor	$\alpha_1 =$	1
Member shape factor	ks =	1
Shrinkage half time	$\tau_s = 190.8t_c^{-0.08}f_{cm28}^{-0.25}[2k_s(V/S)]^2$	
	$\tau_{sh} =$	89.280
Time dependence factor	$E_{cm607}/E_{cm(tc+\tau sh)} = 1.0805/[(t_c+\tau_{sh})/(4 + 0.85\,(t_c+\tau_{sh}))]^{0.}$	
	$E_{cm607}/E_{cm(tc+\tau sh)} =$	1.022
Ultimate shrinkage strain	$\varepsilon_{sh\infty} = -\varepsilon_{s\infty}(E_{cm607}/E_{cm(tc+\tau sh)})$	
	$\varepsilon_{sh\infty} =$	-5.76E-04
Shrinkage time function	$S(t-t_c) = \tanh[(t-t_c)/\tau_{sh}]^{0.5}$	
Shrinkage strains	$\varepsilon_{sh}(t-t_c) = -\varepsilon_{sh\infty}k_h\tanh[(t-t_c)/\tau_{sh}]^{0.5}$	

3.3.1.3 CEB MC90-99 Model

CEB MC 90-99 model is the third model applied to be compared to the measured shrinkage strains.

$$\varepsilon_{sh}(t, t_c) = \varepsilon_{cs0}\beta_s(t - t_c)$$

Where ε_{cso} is the notional shrinkage coefficient, $\beta_s(t - t_c)$ is the coefficient describing the development of shrinkage with time of drying, t is the age of concrete (days) and t_c is the day of the end of moist curing.

Table 9 show some correction factors used in the model for beam # 1. Factors includes a concrete strength factor and ambient relative humidity factor.

The ultimate shrinkage strain was 885 microstrains.

Table 9 Shows shrinkage time function used in CEB model, the model computes autogenous shrinkage and drying shrinkage separately, adding them together gives the total predicted shrinkage for Beam # 1

Shrinkage strains		
Cement type factor	β_{sc} =	5
Concrete strength factor	$\varepsilon_s(f_{cm28}) = [160 + 10\beta_{sc}(9 - f_{cm28}/f_{cmo})] \times 10^{-6}$	
	$\varepsilon_s(f_{cm28})$ =	**6.10E-04**
Ambient relative humidity factc	$\beta_{RH}(h) = -1.055[1-(h/h_0)^3]$ for 0.4<h<0.99	
	$\beta_{RH}(h) = 0.25$ for h>0.99	
	h_0=	1
	$\beta_{RH}(h)$ =	**-1.451**
Notional shrinkage coefficient	$\varepsilon_{cso}=\varepsilon_s(f_{cm28})\beta_{RH}(h)$	
	ε_{cso}=	-8.85E-04
Shrinkage time function	$\beta_s(t-t_c)= [\{(t-t_c)/t_1\}/\{350([(V/S)/(V/S)_0]^2+(t-t_c)$	
	t_1(days) =	1
	$(V/S)_0$ (in.) =	2
shrinkage strains:	$\varepsilon_{sh}(t,t_c)= \varepsilon_{cso}\beta_s(t-t_c)$	

3.3.1.4 GL2000 Model

The GL model developed by (Gardner & Lockman, 2001) and made to conform to the ACI model guidelines.

The model requires age of concrete when drying starts, cement type, volume to surface ratio and concrete mean compressive strength at 28 days.

$$\varepsilon_{sh}(t, t_c) = \varepsilon_{shu}\beta(h)\beta(t - t_c)$$

Where ε_{shu} is the ultimate shrinkage strain, $\beta(h)$ is the correction factor for the effect of humidity and $\beta(t-t_c)$ is a correction term for the effect of time drying.

Table 10 shows the correction factor for humidity, the resulting ultimate design strain was 730 microstrains.

Table 10 Shows shrinkage time function used in GL2000 model for beam # 1.

Shrinkage strains $\varepsilon_{sh}(t,t_c)$:		
Cement type factor	k =	1.000
Ultimate shrinkage strain	$\varepsilon_{shu} = 900k[4350/f_{cm28}]^{0.5}x10^{-6}$	
	ε_{shu} =	7.36E-04
Ambient relative humidity factor	$\beta(h) = [1-1.18h^4)$	
	$\beta(h)$ =	0.970
Shrinkage time function	$\beta(t-t_c)= [(t-t_c)/(t-t_c+77(V/S)^2]\}^{0.5}$	
shrinkage strains:	**$\varepsilon_{sh}(t,t_c)= \varepsilon_{shu}\beta(h)\beta(t-t_c)$**	

Table 11 shows the ultimate shrinkage strain with the correction factor applied to it, 800 microstrains of ultimate shrinkage was computed.

Table 11 Shows shrinkage time function used in GL2000 model for beam # 2

Shrinkage strains $\varepsilon_{sh}(t,t_c)$:		
Cement type factor	k =	1.000
Ultimate shrinkage strain	$\varepsilon_{shu} = 900k[4350/f_{cm28}]^{0.5}x10^{-6}$	
	ε_{shu} =	8.12E-04
Ambient relative humidity factor	$\beta(h) = [1-1.18h^4)$	
	$\beta(h)$ =	0.970
Shrinkage time function	$\beta(t-t_c)= [(t-t_c)/(t-t_c+77(V/S)^2]\}^{0.5}$	
shrinkage strains:	**$\varepsilon_{sh}(t,t_c)= \varepsilon_{shu}\beta(h)\beta(t-t_c)$**	

3.4 Comparing the Results from Laboratory Experimentations with the Results from the Numerical Models

Results obtained from the four models are compared together and to the results obtained from the experimentation on the prototype beams 1 and 2 done in the laboratory.

3.5 Developing Conclusions and Recommendations

Conclusions and recommendations based on analyzing results from numerical models together with the laboratory tests will be discussed in the coming chapters.

CHAPTER IV

RESULTS

4.1 Background

In this chapter, lab tests are discussed in details, results presented and discussed, numerical models used are also discussed and their results are compared to lab tests. Correlation between the lab results, numerical models and the significance shall be discussed in further chapters.

4.2 Concrete Properties of Concrete prisms and deck slabs

As discussed in the study methodology, concrete properties were tested according to ASTM standards. Test results were used as data inputs for numerical models discussed later on.

4.2.1.1 Fresh concrete properties

Fresh concrete properties are represented in tables 12 and 13 for the concrete used to cast Prototype beams 1 and 2.

Table 12 Fresh concrete properties

	Beam # 1	Beam # 2
Air content (%)	2.7	4
Slump (in.)	4.5	9
Unit Weight (lb/ft^3)	154	152
Concrete Temperature (°F)	94.6	96.6

4.2.1.2 Hardened Concrete Properties

The 28 days concrete properties are given in the following table, those are used in the numerical models.

Table 13 Hardened concrete properties

	Beam # 1	Beam # 2
Compressive strength (psi)	6510	5340
Tensile strength (psi)	570	510
Elastic modulus (ksi)	6450	5270

Figure 23 Compressive Strength Vs. Time according to ASTM C39, Mean 28 days strength shows to be equal to 6510 psi and this value will be used in models. the results from the compressive strength testing on concrete used to cast Prototype Beam# 1; testing was performed in accordance to ASTM C39. Tests were performed at 3 hrs, 6 hrs, 12 hrs, 24 hrs, 36 hrs, 48 hrs, 3 days, 4 days, 7 days, 14 day and 28 days.

The test results for C39 are tabulated in the Appendix chapter.

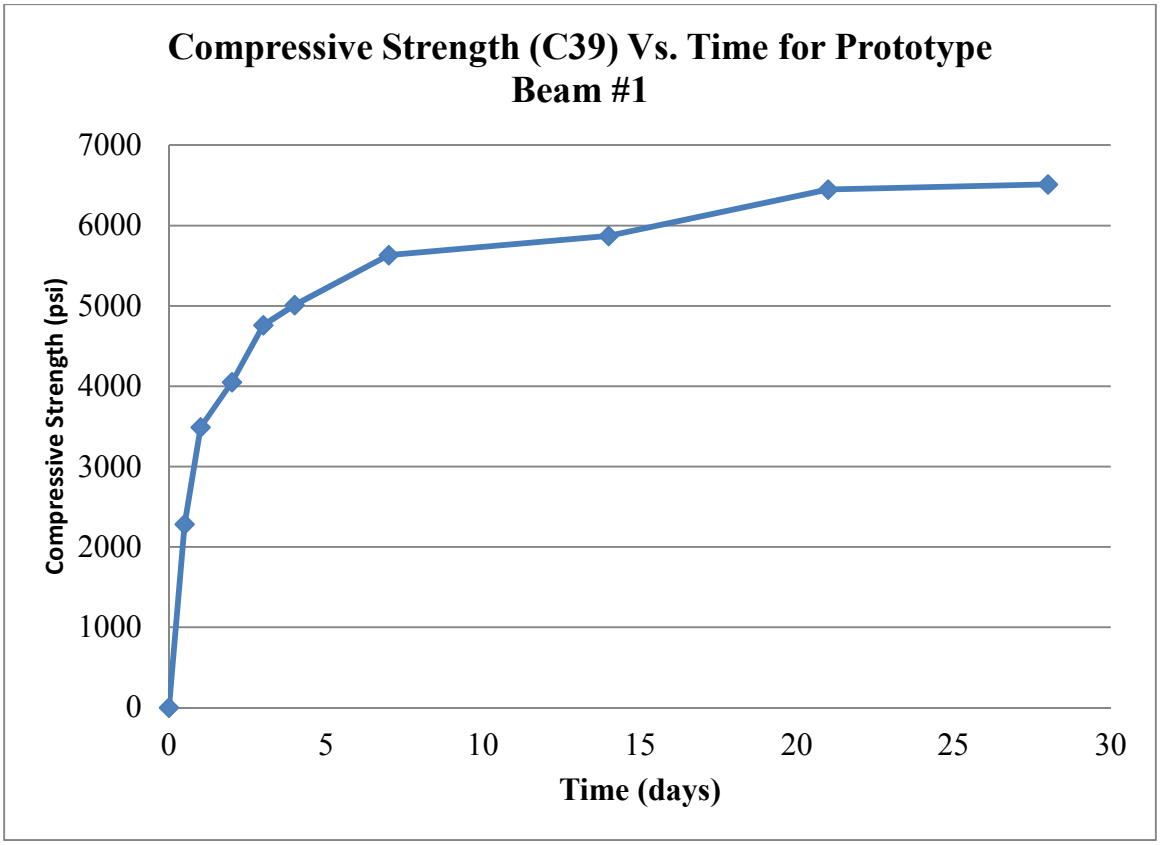

Figure 23 Compressive Strength Vs. Time according to ASTM C39, Mean 28 days strength shows to be equal to 6510 psi and this value will be used in models.

Figure 24 Shows Modulus of Elasticity Vs. Time according to ASTM C469, mean 28 days E is equal to 6444 ksi for prototype beam #1, and this value will be used in the numerical model. represents the results for the Modulus if Elasticity testing on the concrete used to cast Prototype Beam# 1, testing was performed according to ASTM C469 at 3 hrs, 6 hrs, 12 hrs, 24 hrs, 36 hrs, 48 hrs, 3 days, 4 days, 7 days, 14 day and 28

days. The mean modulus of elasticity at 28 days is 6444 ksi and this value is used in the numerical models for Prototype beam# 1.

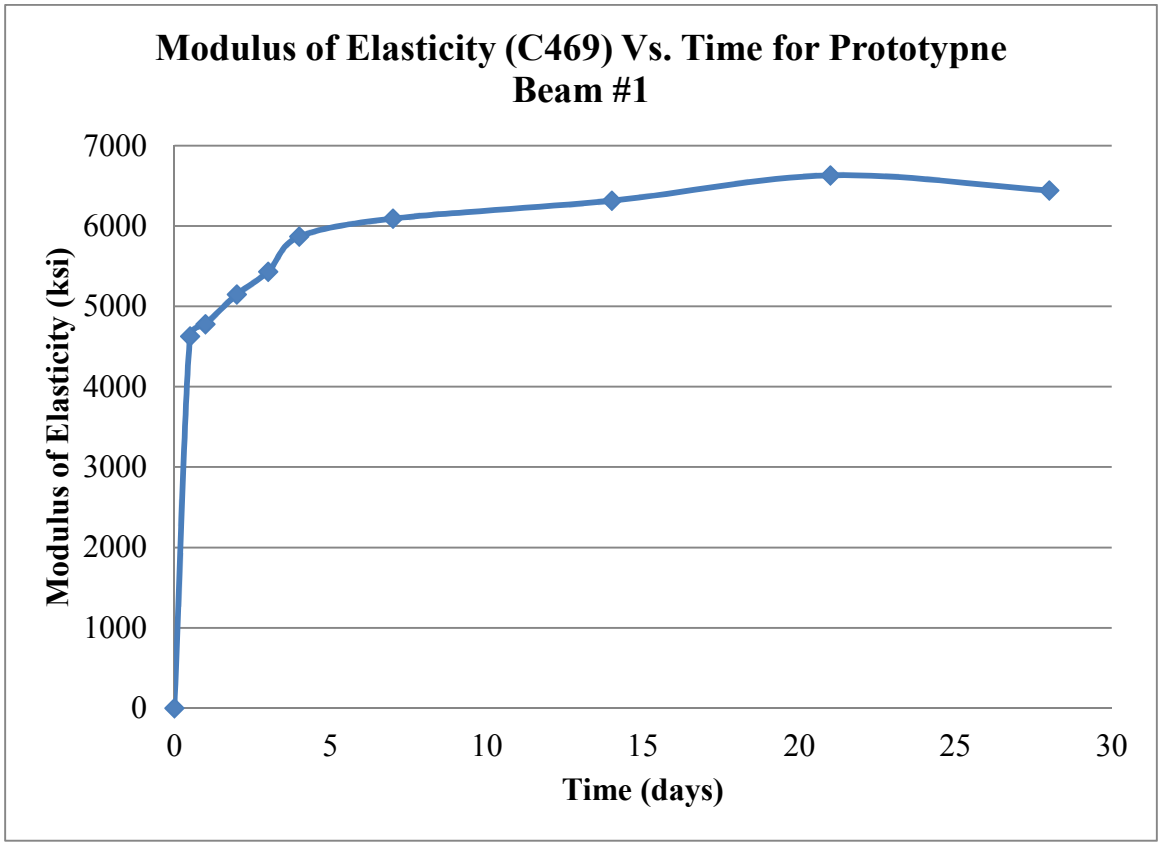

Figure 24 Shows Modulus of Elasticity Vs. Time according to ASTM C469, mean 28 days E is equal to 6444 ksi for prototype beam #1, and this value will be used in the numerical model.

In Figure 25 Splitting Tensile Strength vs. Time according to ASTM C496, Mean 28 days tensile strength was 570 psi which is approximately 9% of the 28 days compressive strength. Tests were performed at 3 hrs, 6 hrs, 12 hrs, 24 hrs, 36 hrs, 48 hrs, 3 days, 4 days, 7 days, 14 day and 28 days. Later figures show the split tensile failure at different concrete ages, at early age the failure is mostly in the concrete paste, after that at older ages the aggregates start to develop failure too.

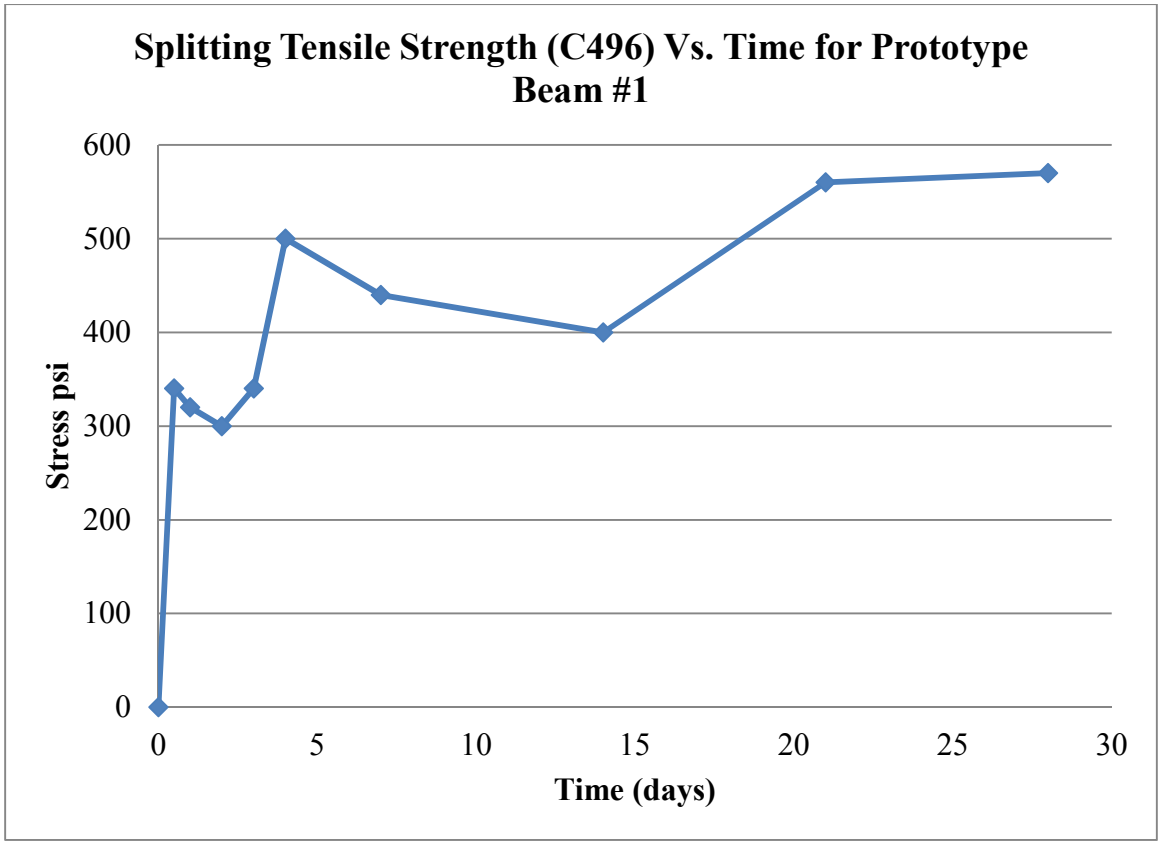

Figure 25 Splitting Tensile Strength vs. Time according to ASTM C496, Mean 28 days tensile strength was 570 psi which is approximately 9% of the 28 days compressive strength.

Figure 26 Tensile Split Failure - 2 Days - Slab 1, failure plane shows to be mainly in the concrete paste.

Figure 27 Tensile Split Failure - 7 Days - Slab 2, failure starts to take place more in aggregates.

4.3 Lab Results for Prototype Beams

Figure 28 Deflection Vs. Time Beam # 1shows the deflection of Prototype beam #1 vs. Time. Time zero is taken as the time when the concrete arrived at the laboratory and when the deck was cast. The deck was cast on 8/28/2014 at 11:40 AM, the zero reading for the deflection before casting the concrete was 0.45 in. The most recent data was taken at an age of 1150 hours which was taken on 10/15/2014 at 8:00 PM. The deflection at mid-spam at this time was 0.096 in. downwards.

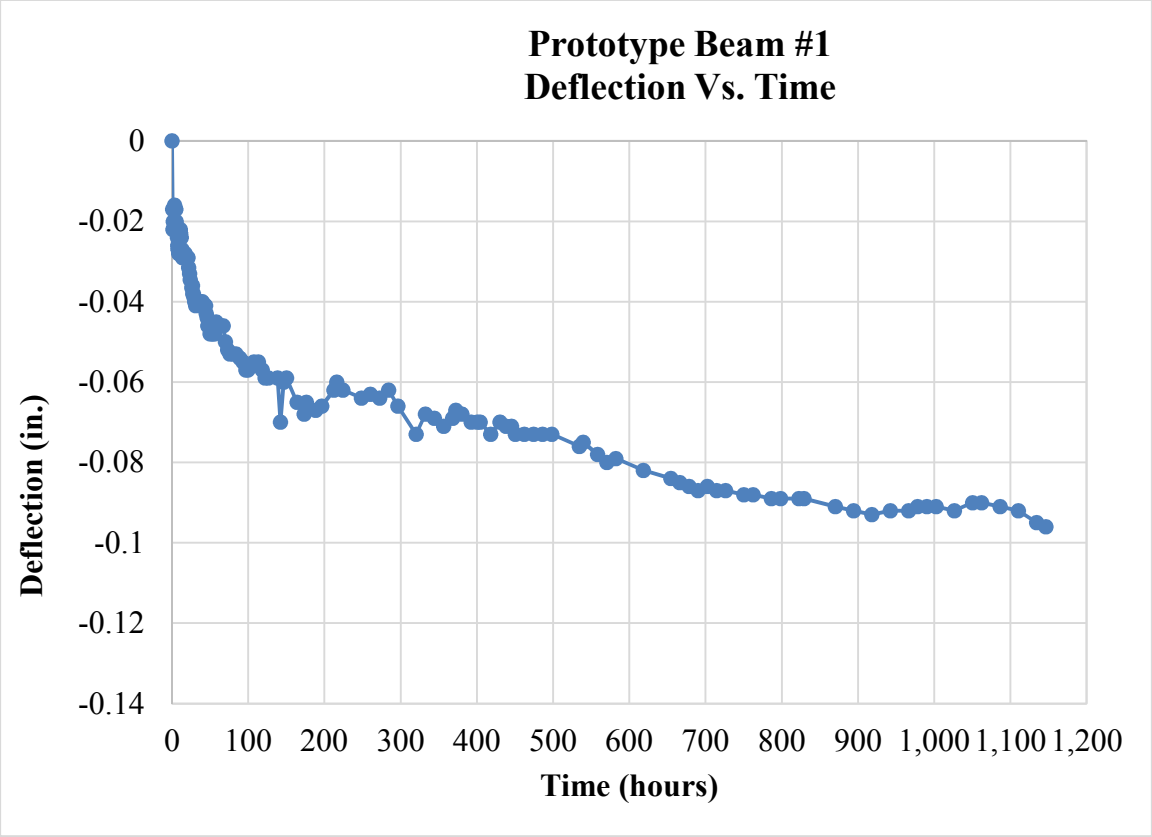

Figure 28 Deflection Vs. Time Beam # 1

Figure 29 Deflection Vs. Time Beam # 2 shows the deflection of Prototype beam #2 vs. Time. Time zero is taken as the time when the concrete arrived at the laboratory and when the deck was cast. The deck was cast on 9/3/2014 at 4:30 PM, the zero reading for the deflection before casting the concrete was 0.40 in. The most recent data was taken at an age of 960 hours which was taken on 9/22/2014 at 8:00 PM. The deflection at mid-spanm at this time was 0.120 in. downwards.

Measured deflection at 60 days maybe represented as 1/1500

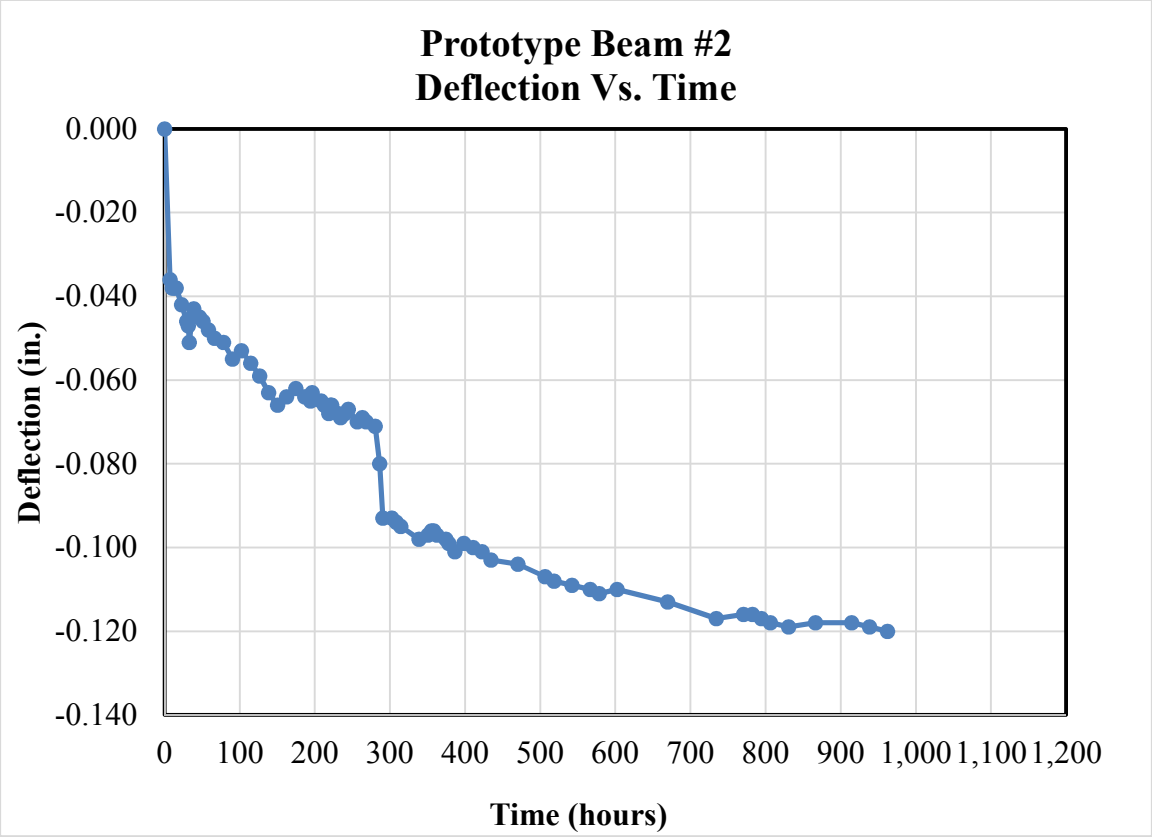

Figure 29 Deflection Vs. Time Beam # 2

Direct shrinkage measurements on concrete prisms were taken to measure unrestrained shrinkage strains. The concrete prisms were cast from the ready mix concrete that was used to cast the composite slab atop Prototype Beam ". Figure 30 Average and Median Strains vs. Time – All specimens – Beam #1, Note the median compressive strain is about -450 microstrains. shows the average and median strains vs. time for the four specimens of Beam# 1, while Figure 31 Average and Median Strains vs. Time – All specimens – Beam #2. Note the median compressive strain is about -350 microstrains. shows the same for Beam# 2. Reading were taken from two sides of each of the four prisms for each prototype; that's to say each data point represents the average of 8 readings.

Measured deflection at 40 days can be represented as 1/1225

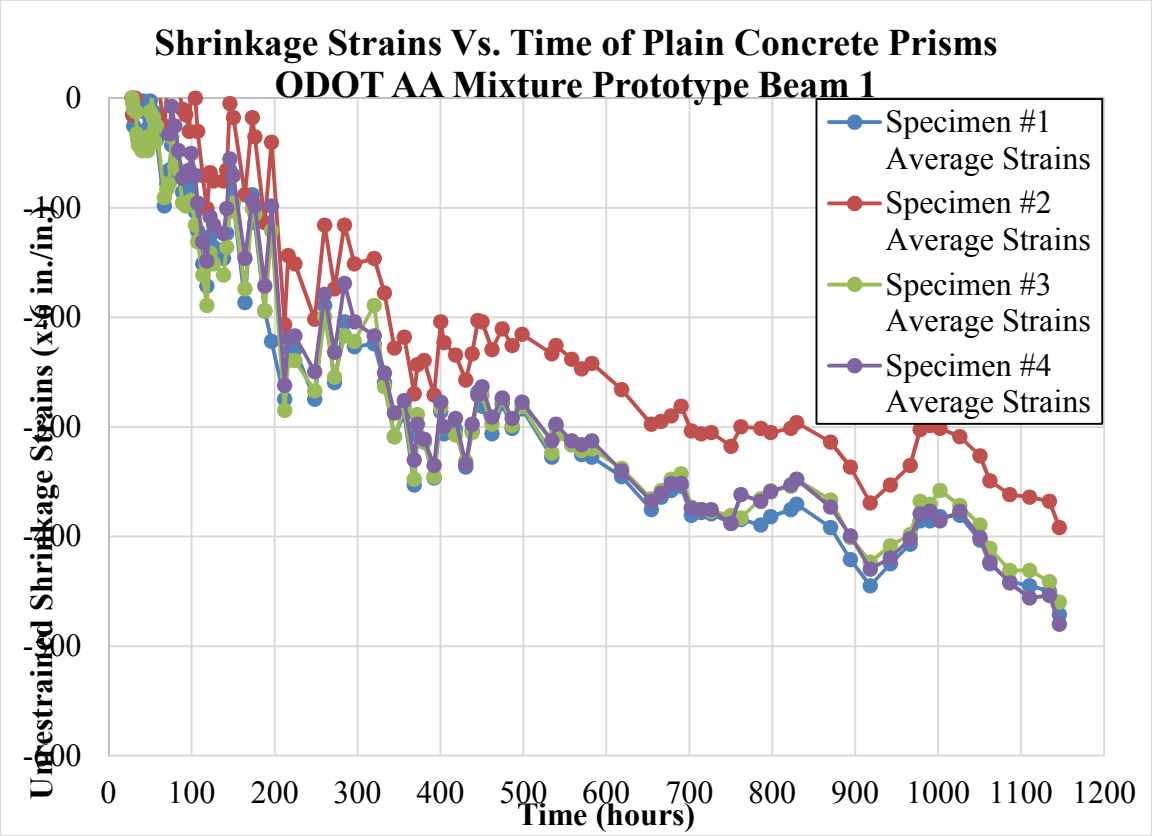

Figure 30 Average and Median Strains vs. Time – All specimens – Beam #1, Note the median compressive strain is about -450 microstrains.

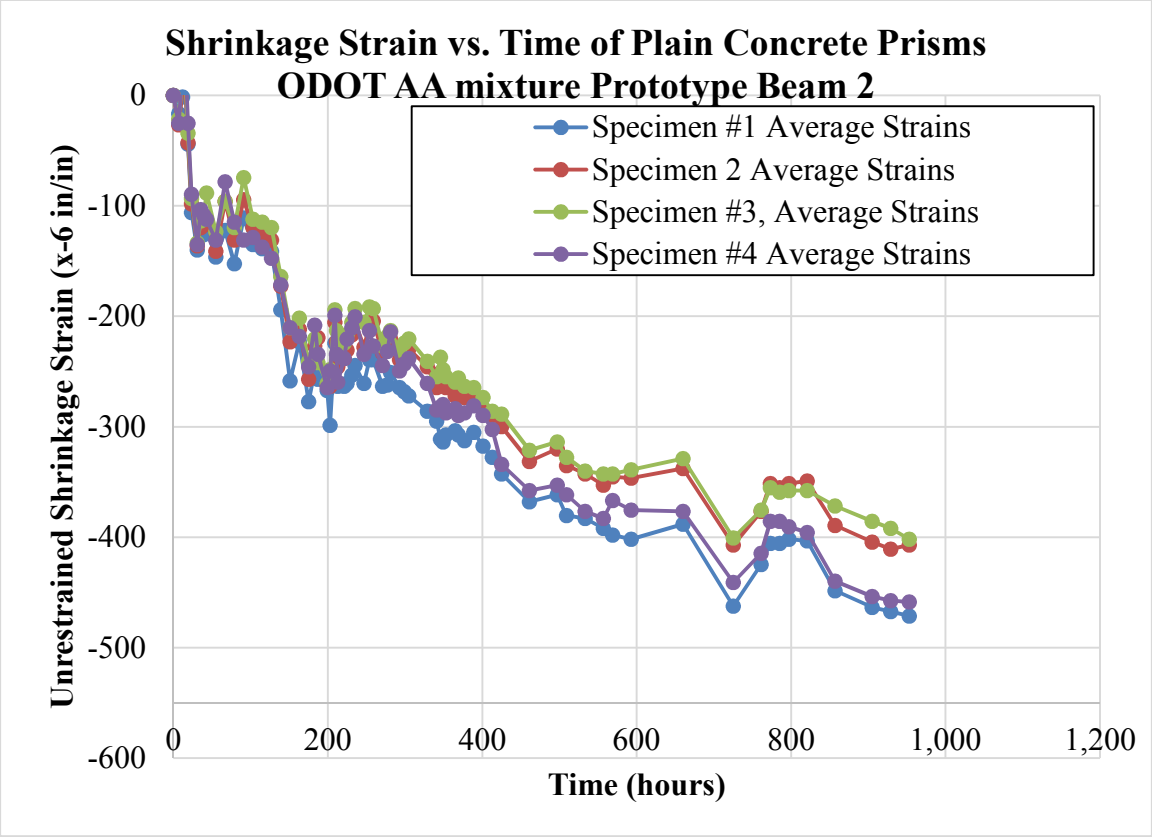

Figure 31 Average and Median Strains vs. Time – All specimens – Beam #2. Note the median compressive strain is about -350 microstrains.

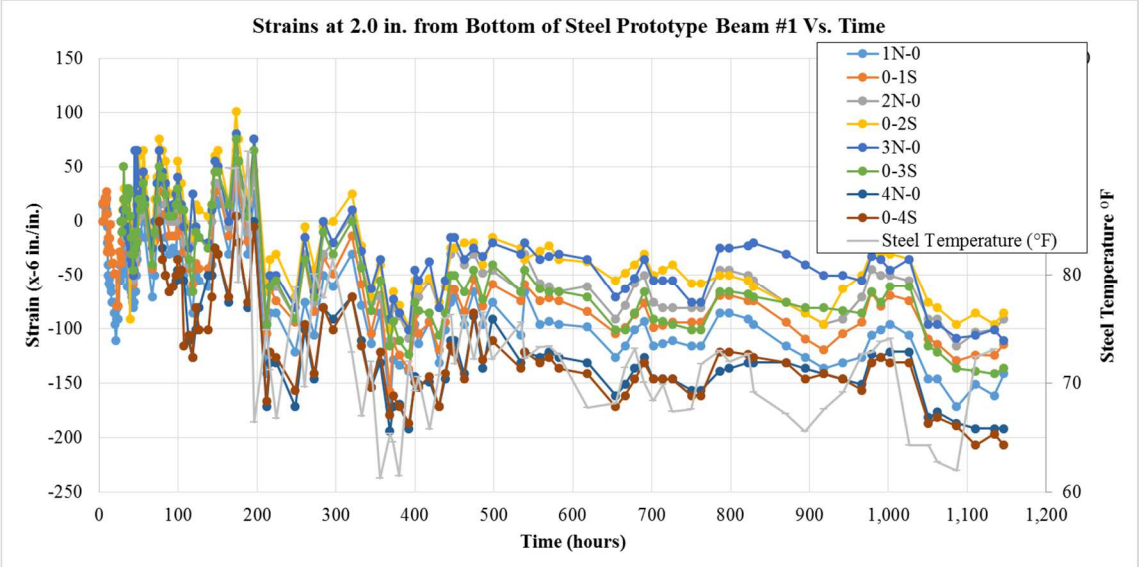

Figure 32 Measured steel strains at 2 in. up from the bottom of the steel beam, Prototype Beam #1. The median value of strain in the steel is about -140 microstrains.

From Figure 32 Measured steel strains at 2 in. up from the bottom of the steel beam, Prototype Beam #1. The median value of strain in the steel is about -140 microstrains., the steel strains shows to be consistent with the temperature changes, steel temperatures changes from 90 F to approximately 70F, then approximately 130 microstrains can be attributed to the change in temperature and not necessarily strains caused by restraining the concrete deck. The median value for beam# 2 was approximately -140 microstrains.

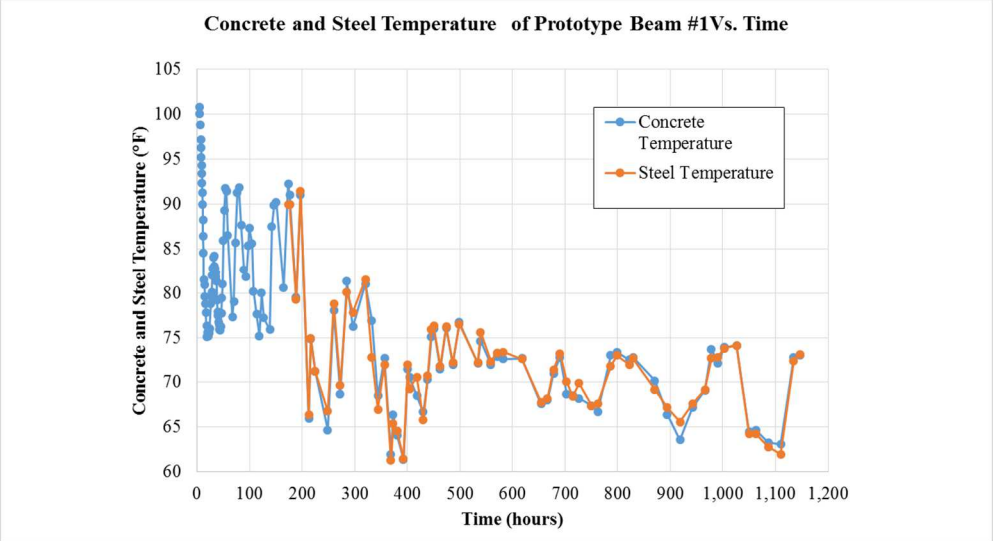

Figure 33 Another graph that shows the changes in temperature to be matching the strains measured in the steel beam at 2 in. from the bottom for Beam# 1.

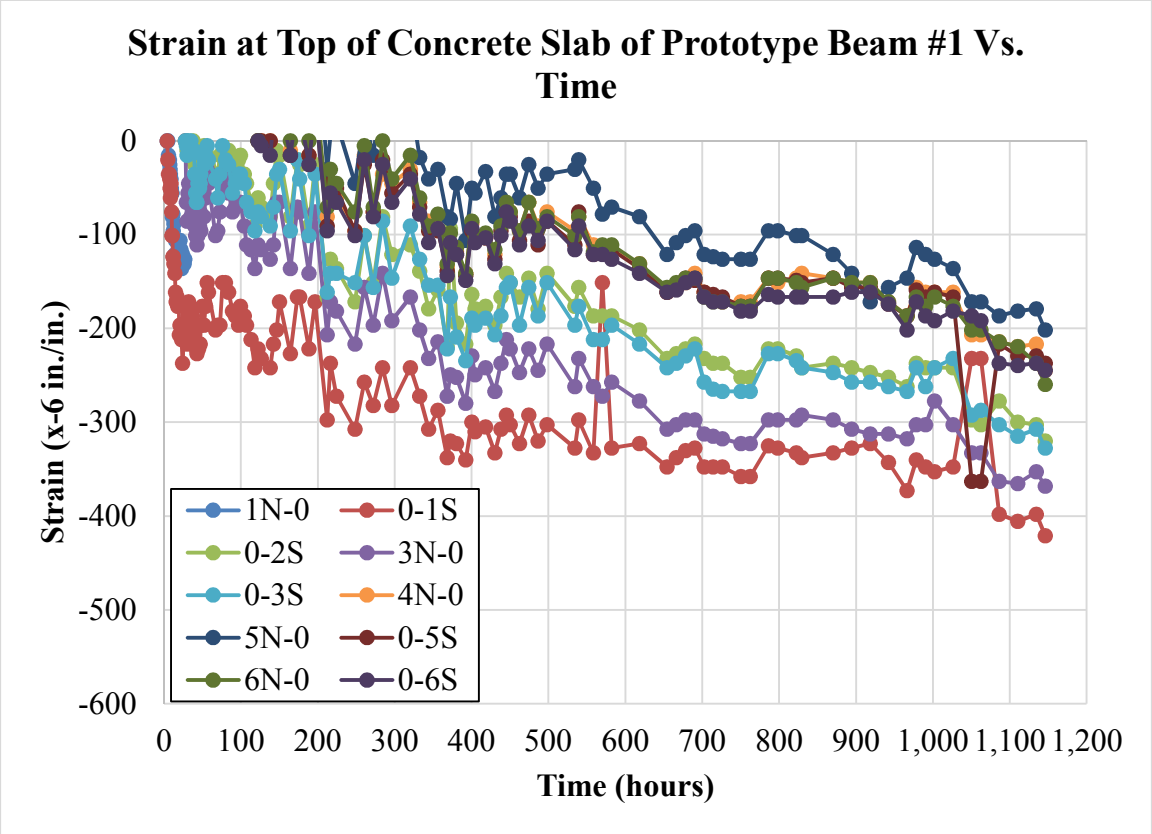

Figure 34 Concrete Strains measured on the top of the concrete slab for Prototype Beam #1. Strains were measured in multiple locations and show increasing compressive strain over time. The median value is about -300 microstrains

The median for the compressive strains shown in Figure 34 Concrete Strains measured on the top of the concrete slab for Prototype Beam #1. Strains were measured in multiple locations and show increasing compressive strain over time. The median value is about -300 microstrains be then compared to the strains calculated using the numerical models. This continuous shortening over time can be a reason for downward deflection in the composite beam.

4.4 NUMERICAL MODELS FOR PREDICTING SHRINKAGE

4.4.1.1 ACI 209R-92 Model

Figure 35 shows a comparison between the measured vs. predicted shrinkage strains over time using the ACI 209R-92 model.

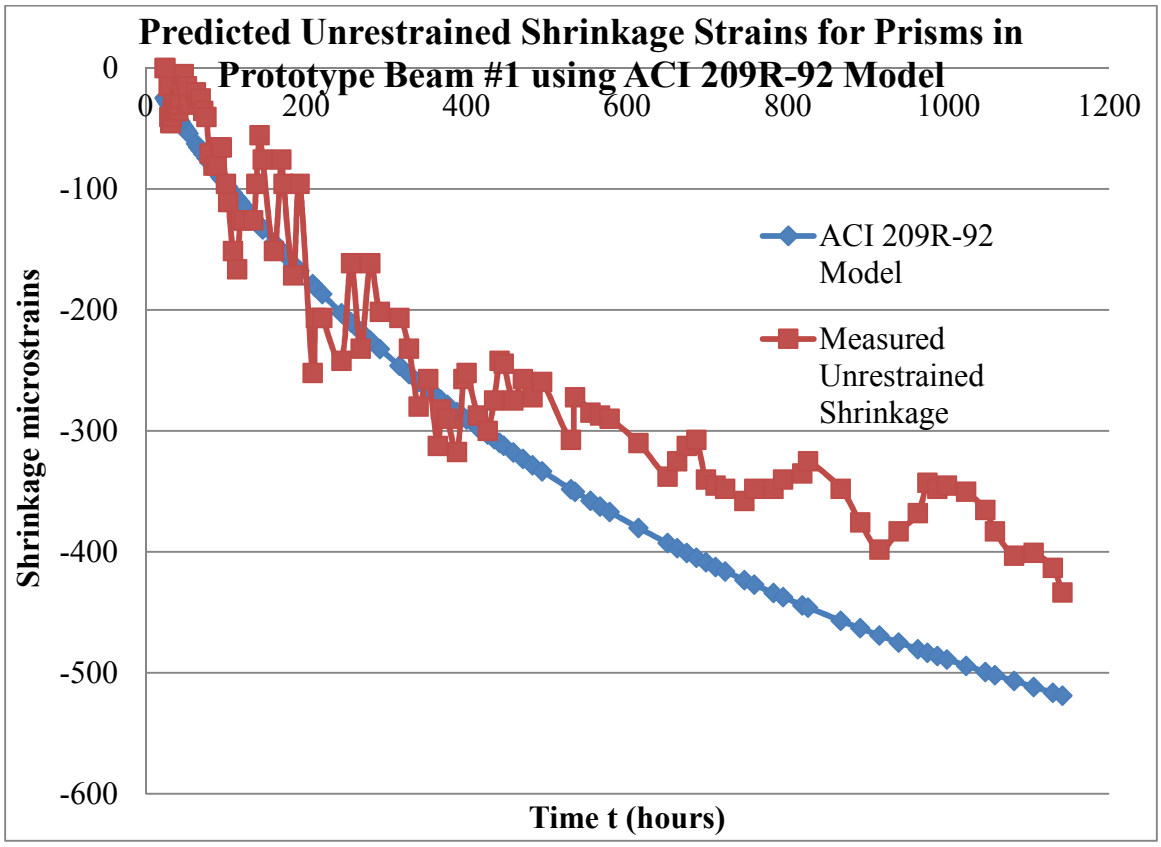

Figure 35 Predicted unrestrained shrinkage strains for prototype beam # 1 using ACI 209R-92 Model compared to the average measured unrestrained direct shrinkage measured from the prisms of beam # 1, the graph shows that ACI model makes a good fit to the measured data.

Then in figure 36, making use of mechanics of materials, the deflection at the mid-span of the composite beam is predicted and plotted. In the graph it shows a comparison between the predicted and measured deflection at mid-span for beam#1 using the ACI 209 model.

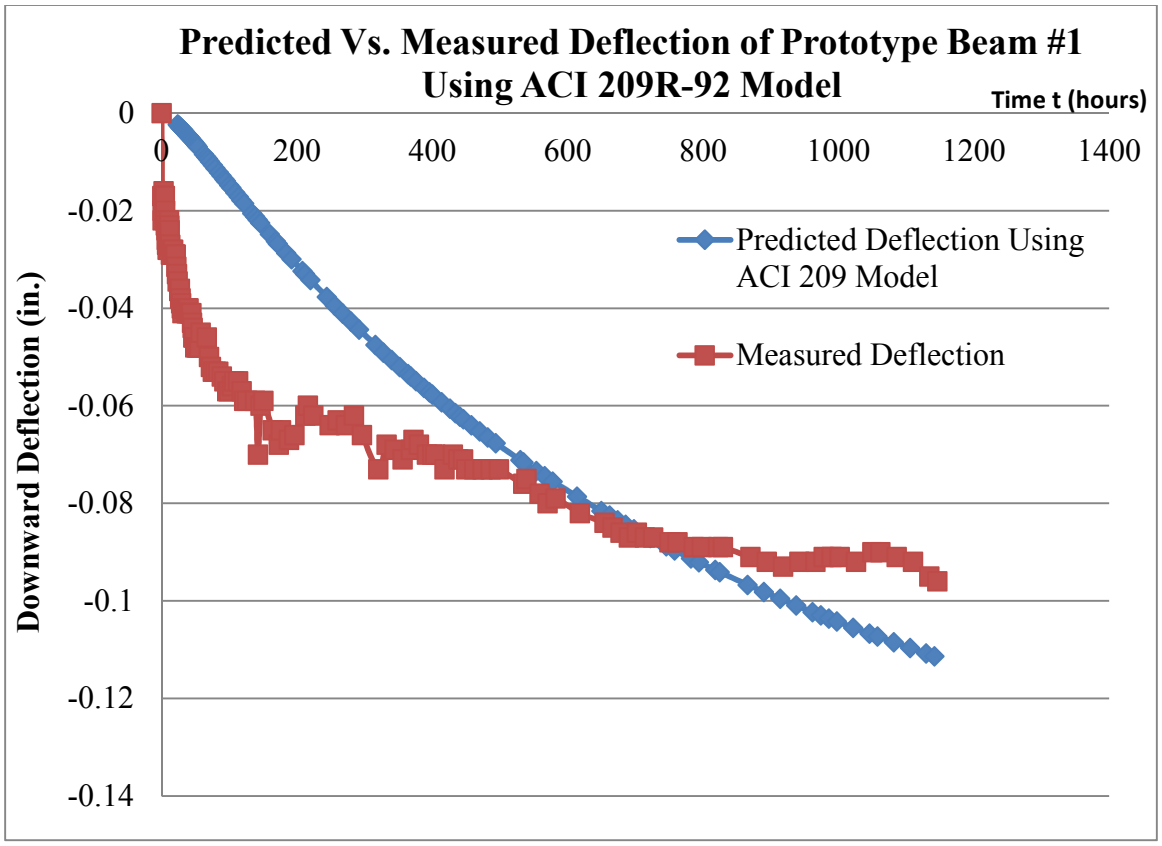

Figure 36 Predicted mid-span deflection due to restrained strains compared to measured mid-span deflection for prototype beam # 1, the predicted values show to be way off the measured value, at 50 days the predicted deflection was 0.25 in downwards whereas the measured one was 0.075 in. downwards.

The following figures show the predicted and measured shrinkage strains for Prototype Beam# 2 usning the ACI model, the deflections are then calculated in the same manner as beam# 1 and compared to the measured values at the mid-span.

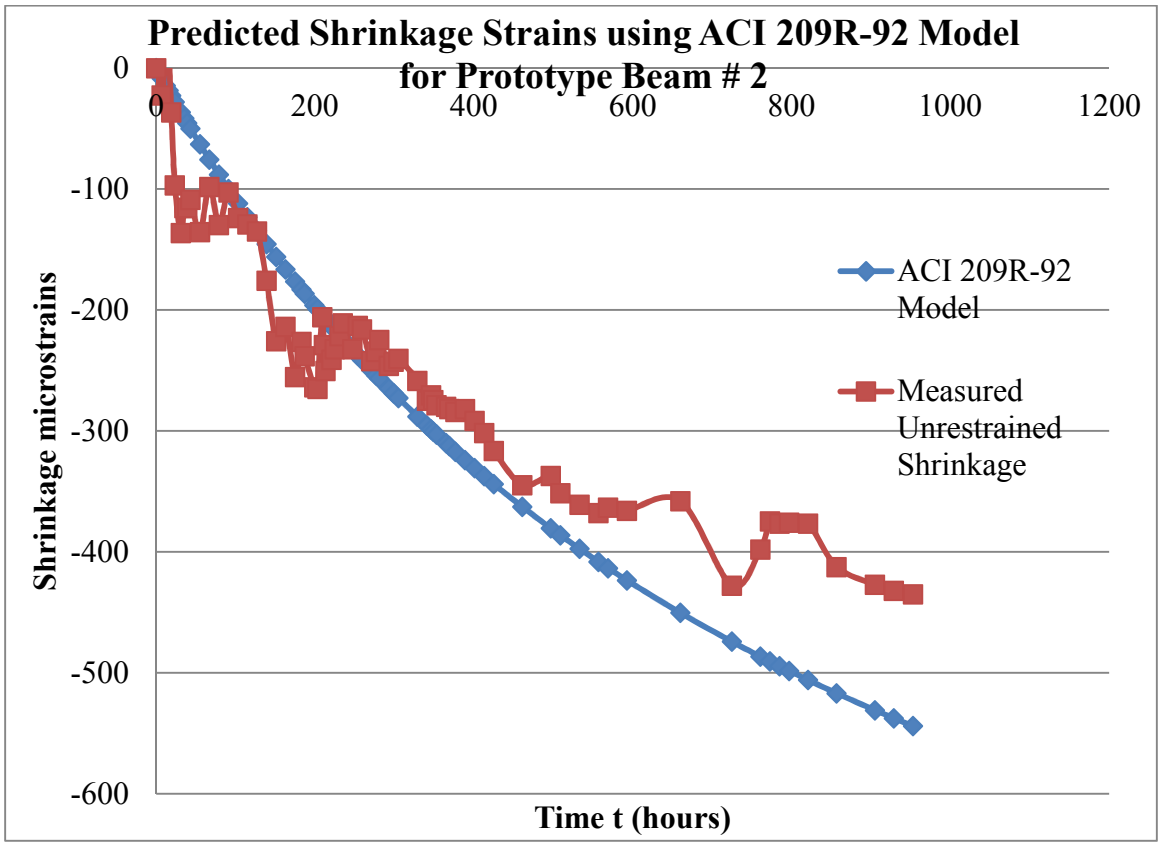

Figure 37 Predicted shrinkage strains of Prototype Beam # 2 vs. time using the ACI shrinkage model

Using the predicted shrinkage strains values and applying the theoretical method shown in the study methodology, the deflection was predicted as shown in figure 38.

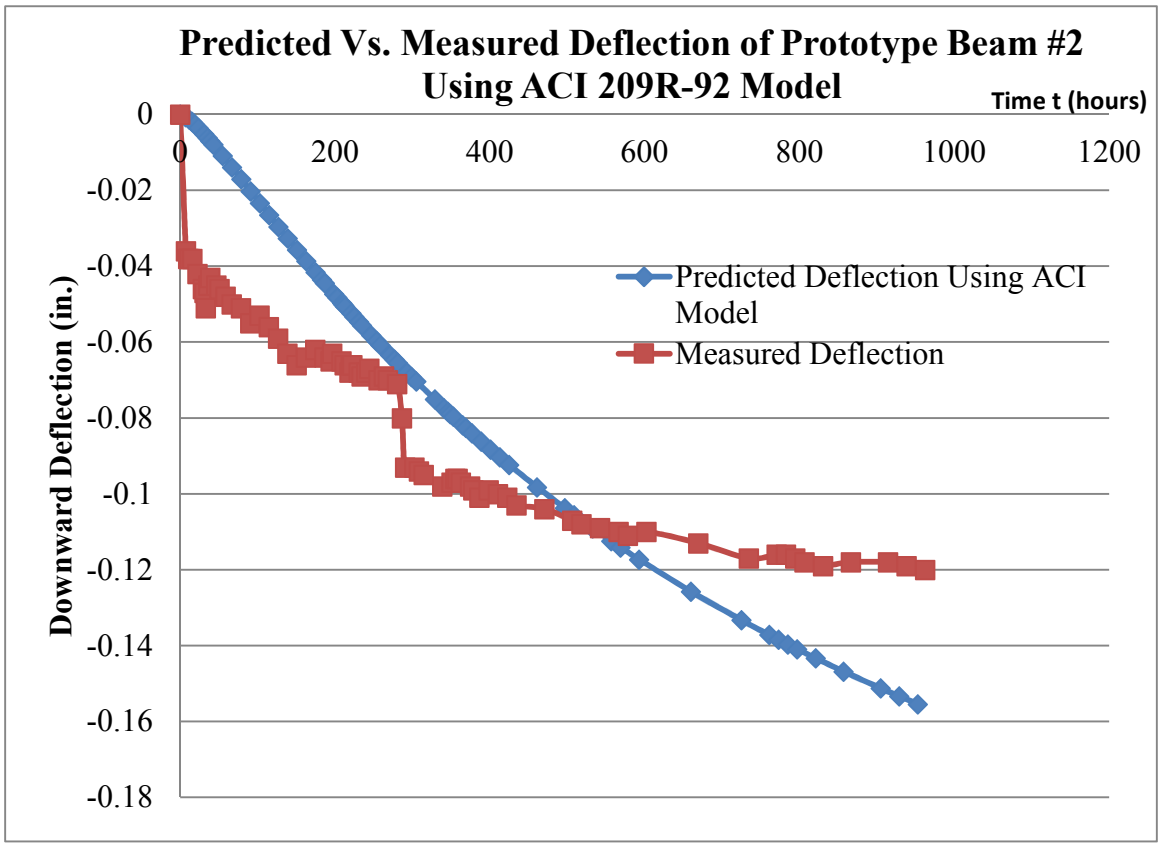

Figure 38 Predicted vs. measured deflection over time for Prototypbe Beam# 2 using the ACI shrinkage model. Data were collected for 1200 hours.

4.4.1.2 Bazant Baweja B3 Model

The following figures show a comparison between the predicted shrinkage strains for both Prototype Beam 1 and 2 with the measured strains. Then using simple mechanics of materials the deflections at mid-span were computed and also compared to the deflection readings from the lab.

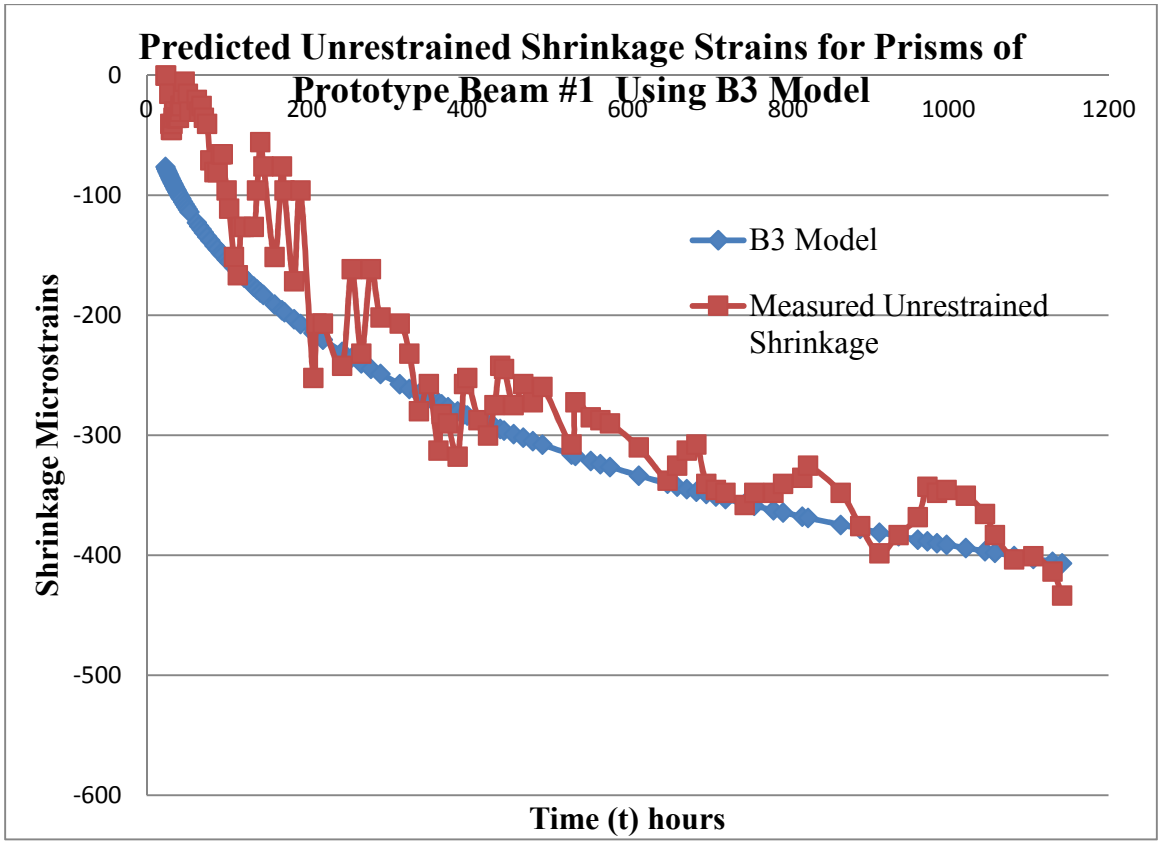

Figure 39 Predicted shrinkage strains over time compared to measured shrinkage strains.

Time dependent modulus of elasticity was used in the 4 models, it is based on the B3 model originally but I made use of it in all models for more accurate results.

Figure 40 show a comparison between the tested values for the elastic modulus and the values computed using the time dependent equation given by the B3 model.

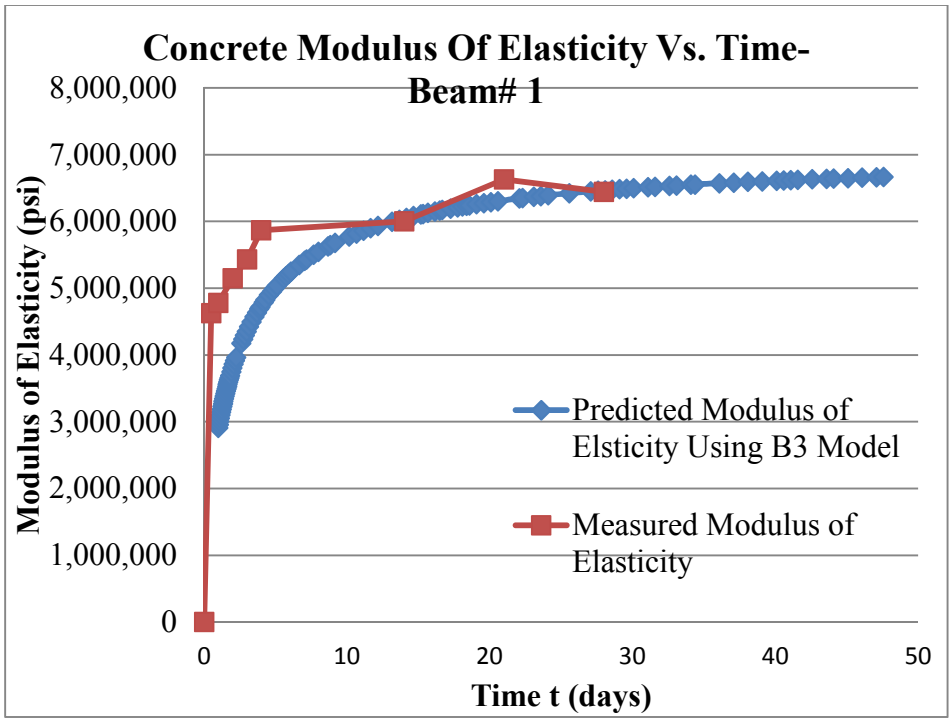

Figure 40 Predicted vs. Measured modulus of elasticity over time for Prototype Beam#1

Figure 41 shows the measured vs. predicted deflection using B3 model, graph is for beam # 1.

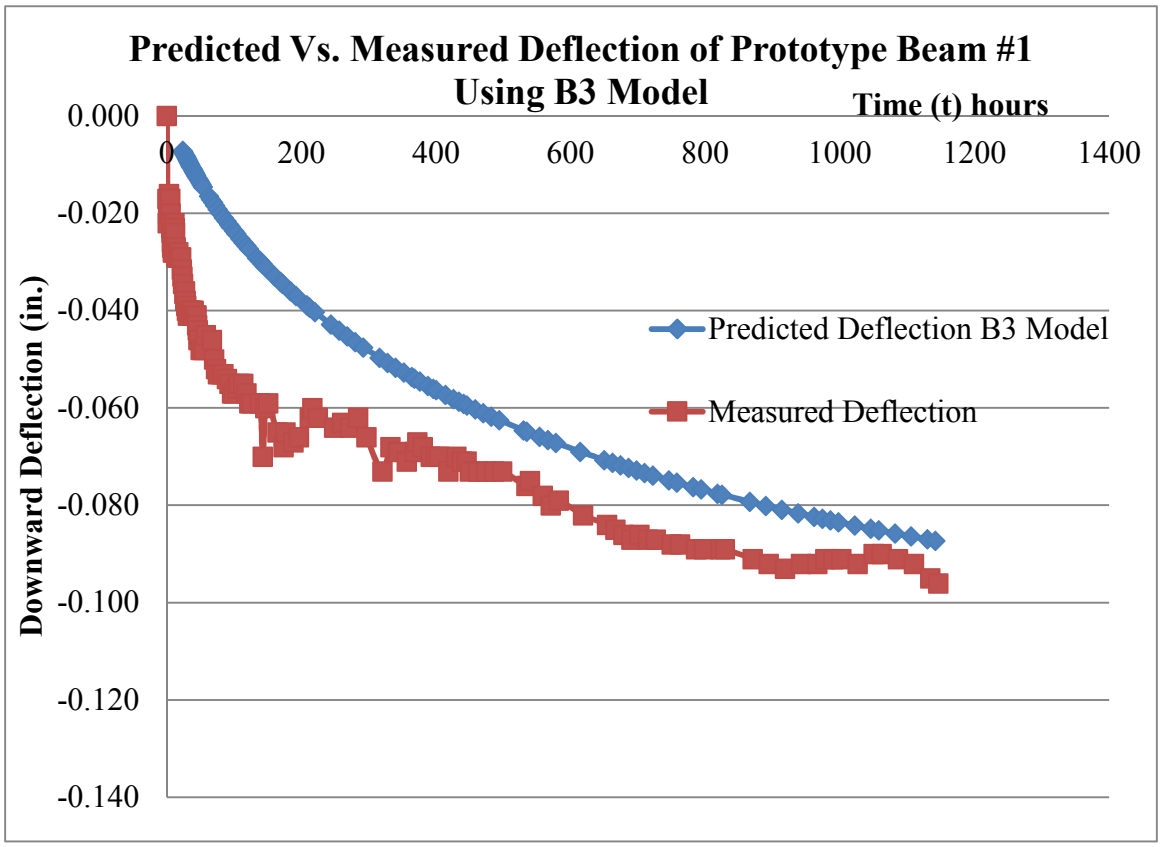

Figure 41 Computed vs. measured deflection for Prototype beam # 1 using B3 model

Figure 42 shows the predicted unrestrained shrinkage for beam # 2 opposed to the measured unrestrained strains. Then figure 43 shows the estimated vs. measured elastic modulus using the B3 model followed by the predicted vs. measured deflection for prototype beam # 2.

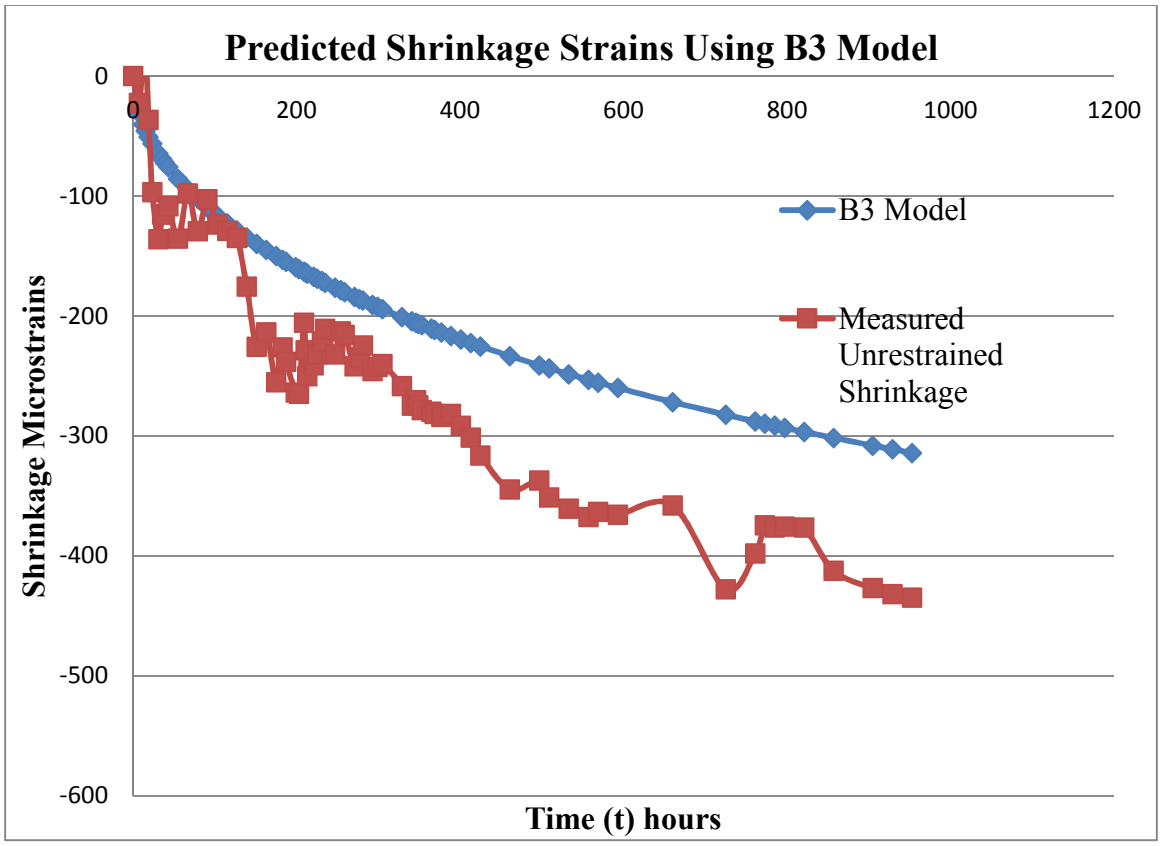

Figure 42 Computed vs. measured shrinkage strains for Prototype beam # 2 using B3 model

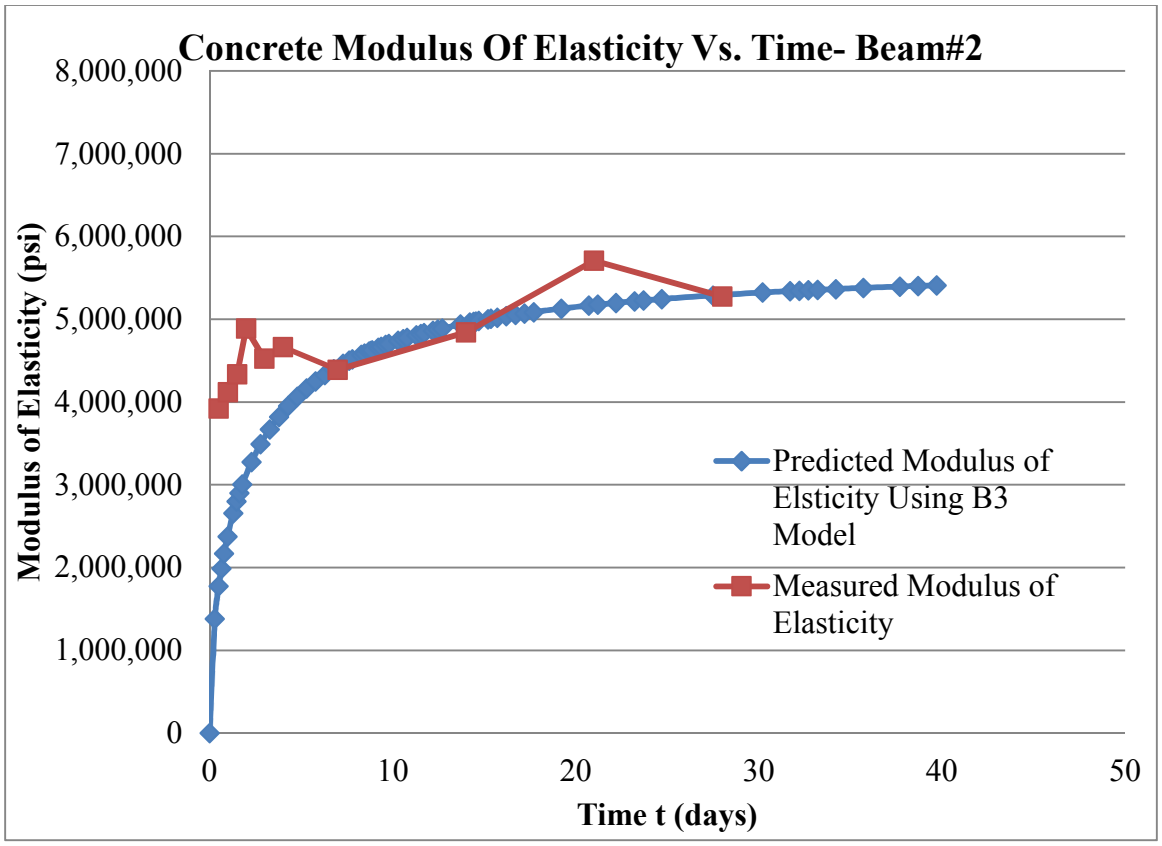

Figure 43 Predicted Elastic Modulus using B3 model compared to the actual tested elastic modulus, at early ages actual elastic modulus is higher than the predicted one, this is attributed to the fact that the elastic modulus is highly dependent on aggregates, so most of it develop from day one.

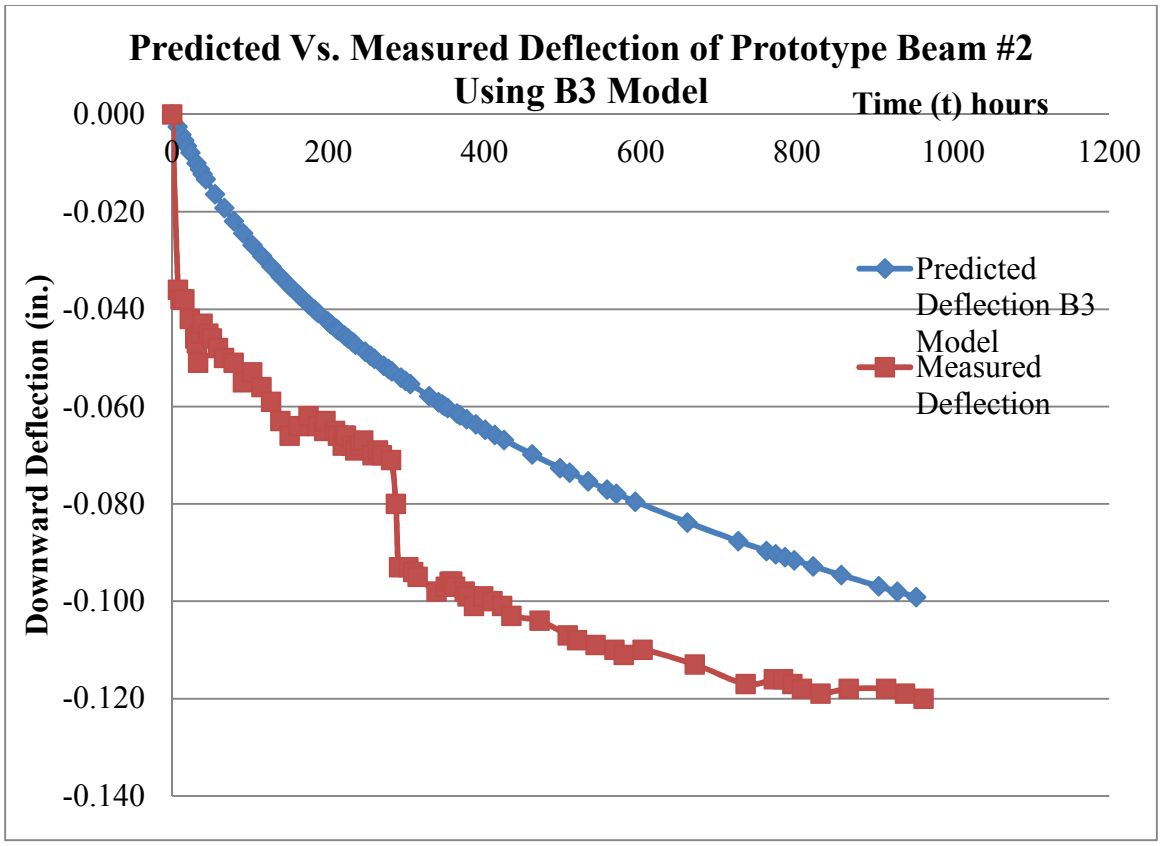

Figure 44 B3 model seems to predict shrinkage to a very minimal amount of error.

4.5 CEB MC90-99 Model

The following chart show the predicted shrinkage strains using the CEB model, the shrinkage stains are subdivided into Autogenous and drying, adding both of them gives the total shrinkage strain.

Figure 45 shows the different types of predicted shrinkage strains together with the total for prototype beam# 1

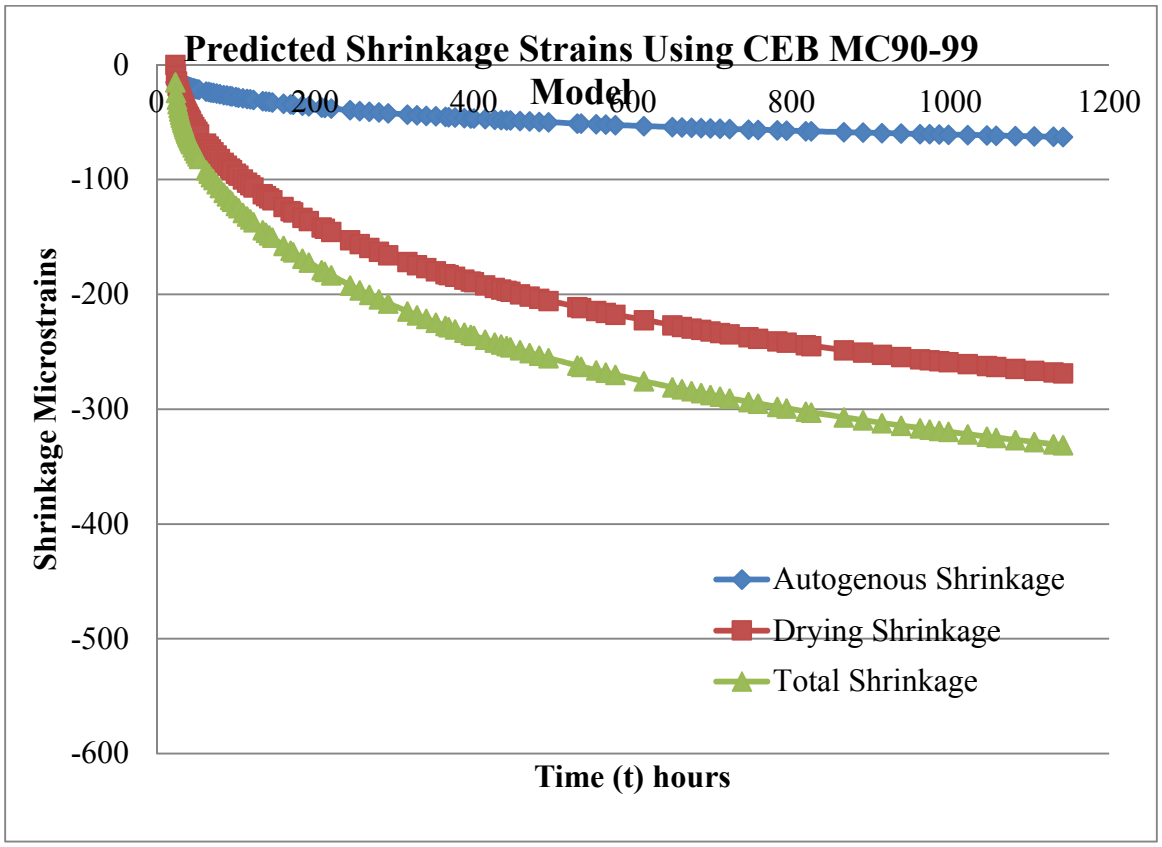

Figure 45 CEB model subdivides total shrinkage into autogenous shrinkage and drying shrinkage, model shows that autogenous shrinkage form a small proportion of total shrinkage, graph shows values for Beam # 1.

Figure 46 shows just the total predicted shrinkage strains compared to the measured values. While figure 47 shows the calculated and measured mid-span deflection over time for prototype beam#1.

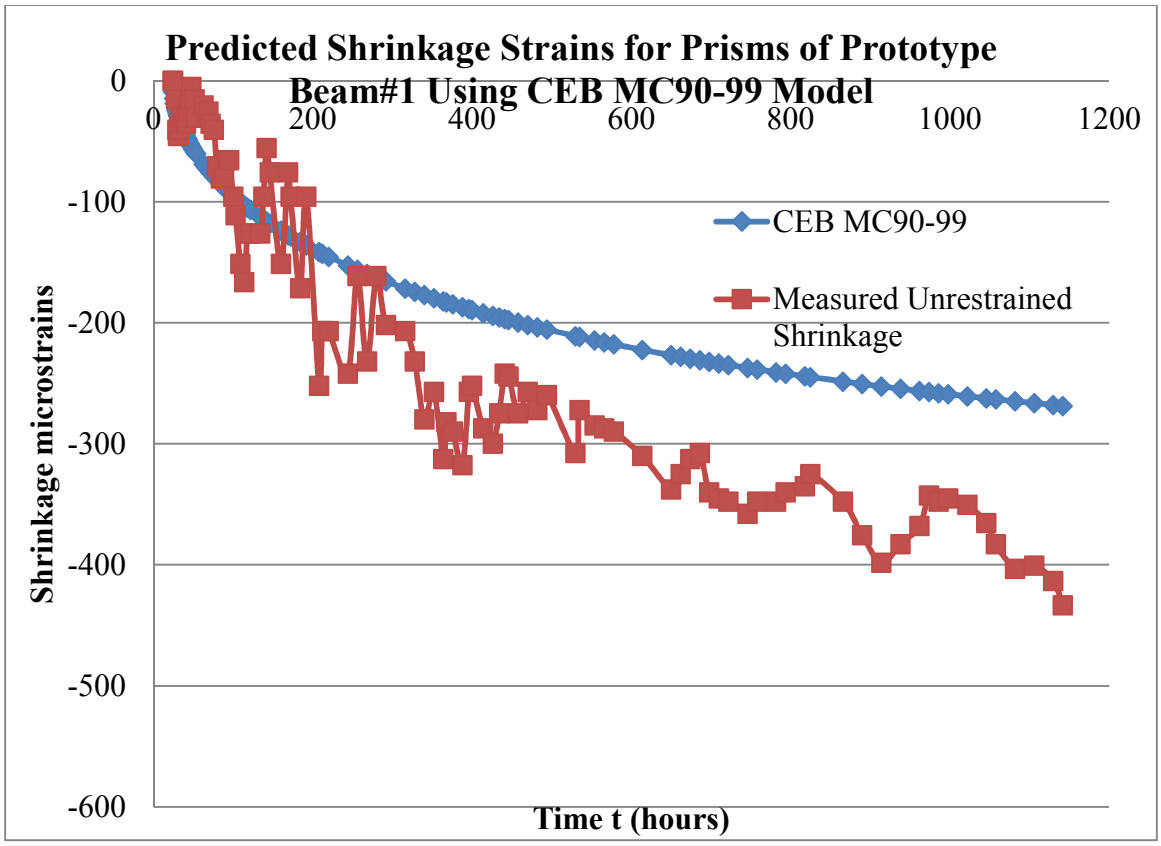

Figure 46 CEB model underestimates predicted shrinkage for beam # 1, error at early age is less compared to the measured strains.

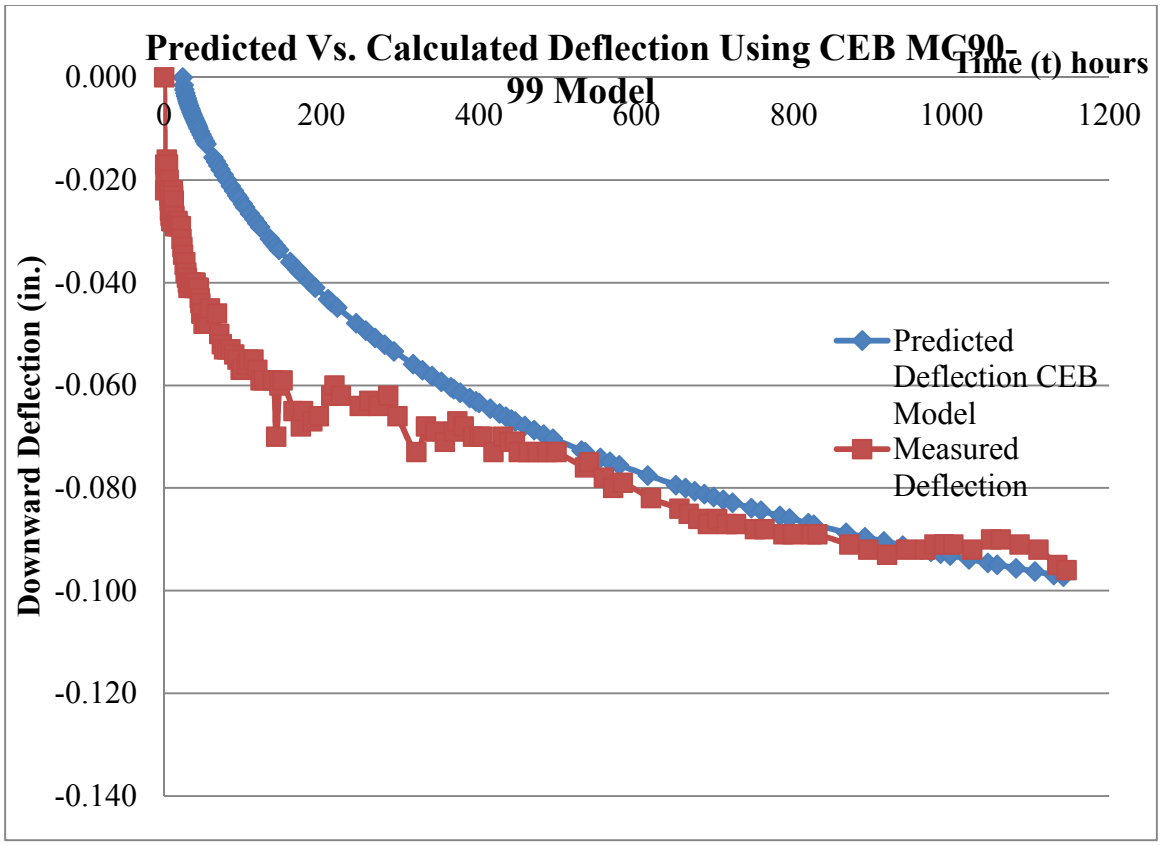

Figure 47 Predicted deflection using CEB Model for beam # 1 shows a good fit for the measured mid-span deflection, at 50 days the model predicted almost the same downward deflection at 50 days.

Figure 48 shows the predicted shrinkage strains using the CEB model as opposed to the measured strains vs. time for prototype beam # 2. Figure 49 shows the predicted and measured deflections for the same beam using the CEB model.

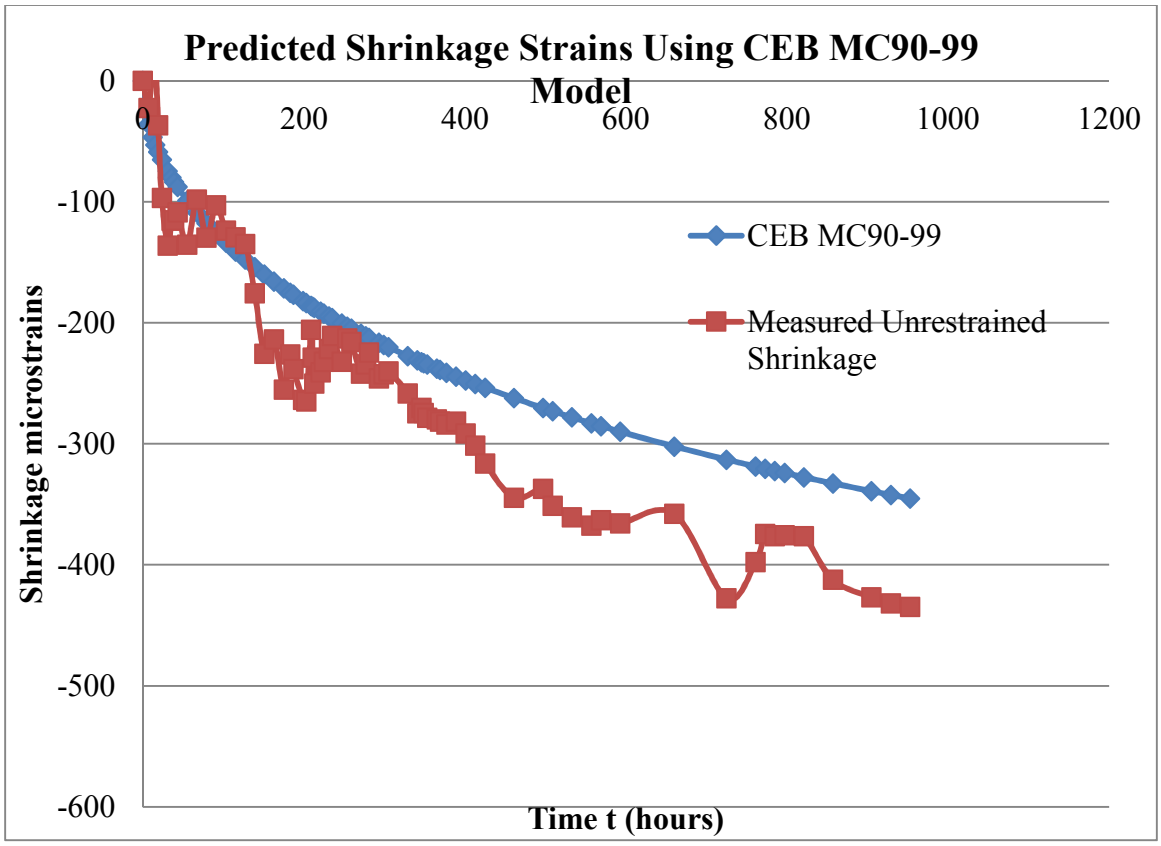

Figure 48 Predicted Vs. measured shrinkage strains using CEB model for beam # 2

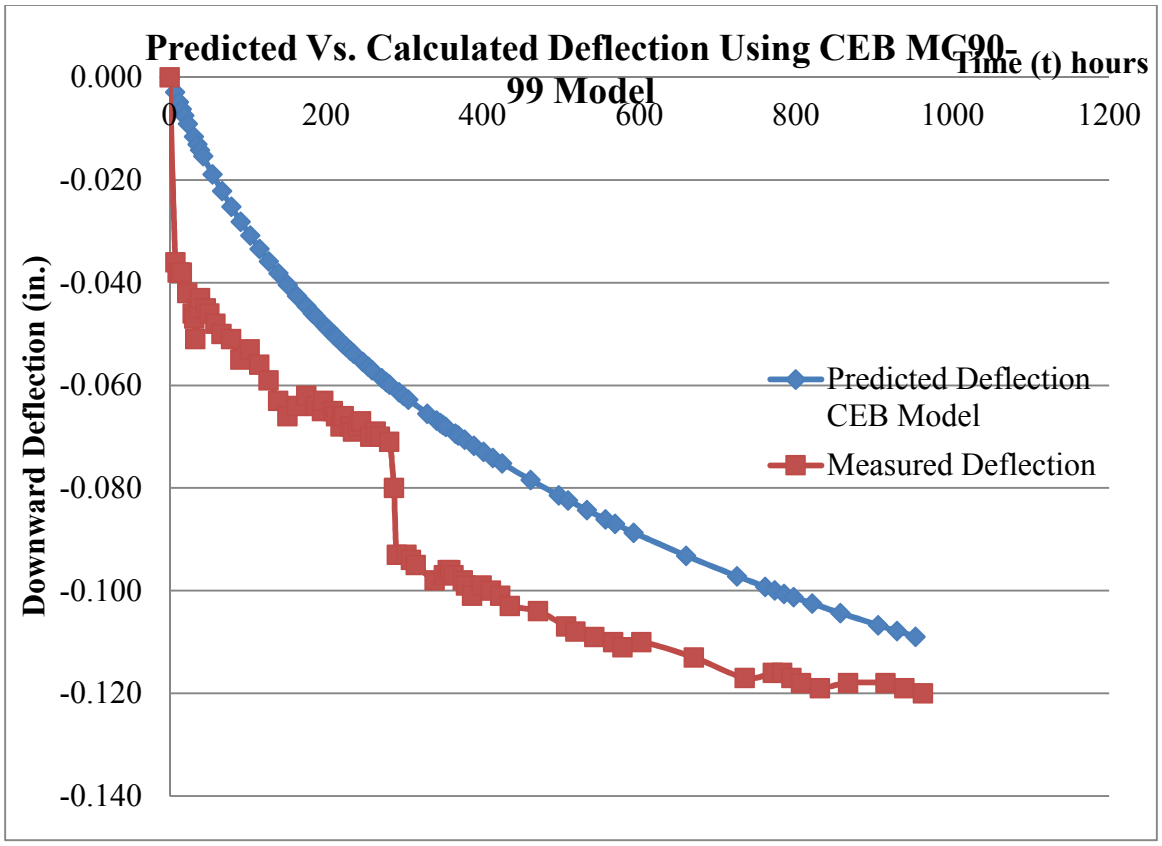

Figure 49 The model this time show a very minimal error compared to beam # 1, although same model was used but for beam # 2

4.6 GL2000 Model

The following charts show the predicted vs. the measured shrinkage strains for Prototypes # 1 and # 2. Also the expected vs. measured deflections at mid-spans of the prototypes are shown.

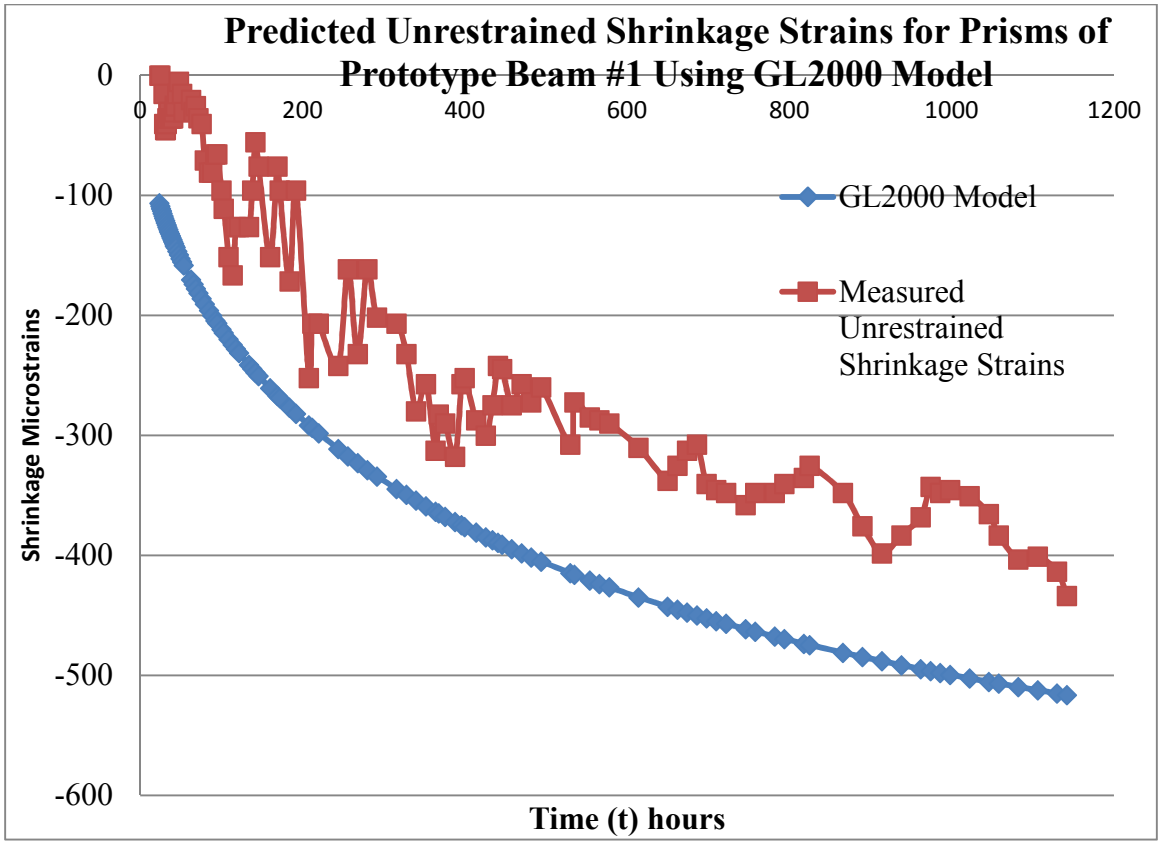

Figure 50 The GL2000 being very good at expecting shrinkage strains for beam # 2, this error making the curve not fit I attribute it to some inputted concrete properties

Figure 51 shows predicted vs. measured deflection for beam # 1.

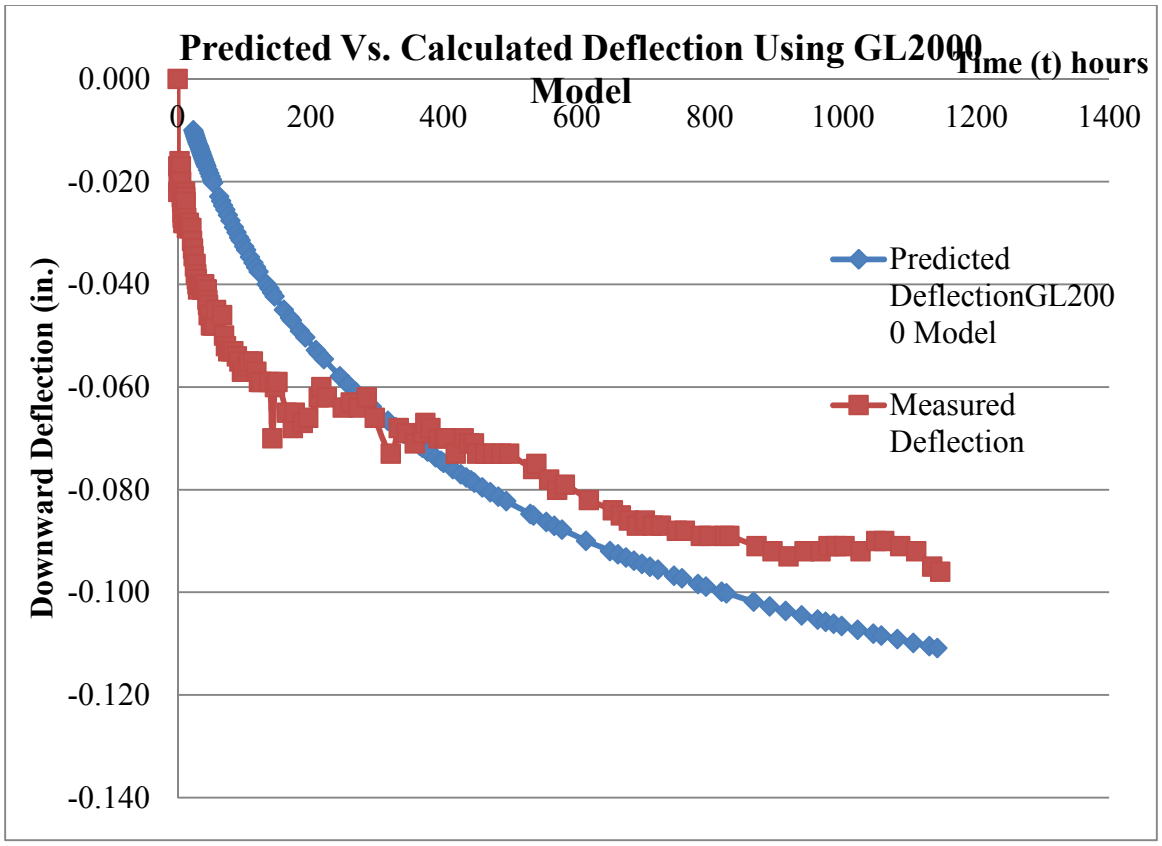

Figure 51 Predicted vs. calculated deflection for beam# 1

Similar shrinkage strains and deflections for beam # 2 are shown in figures 52 and 53.

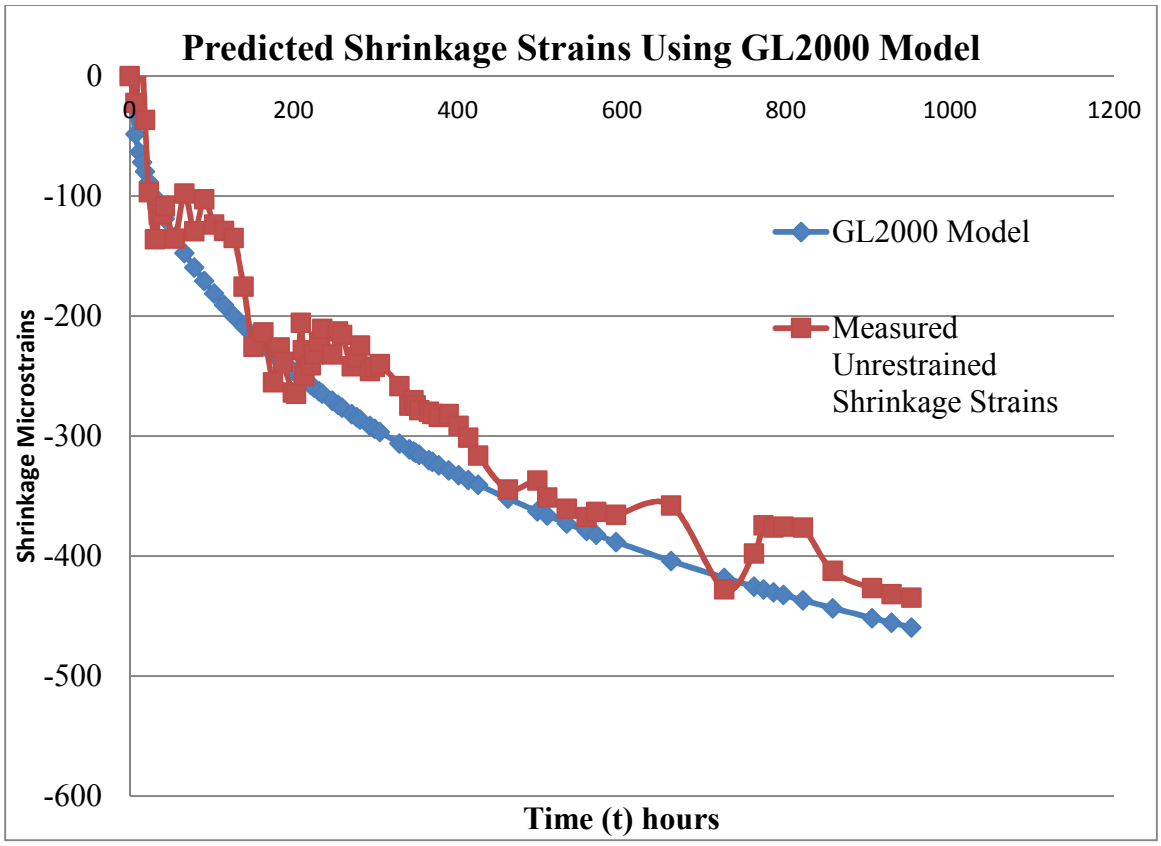

Figure 52 GL model seems to be a good model for predicting shrinkage for beam # 2

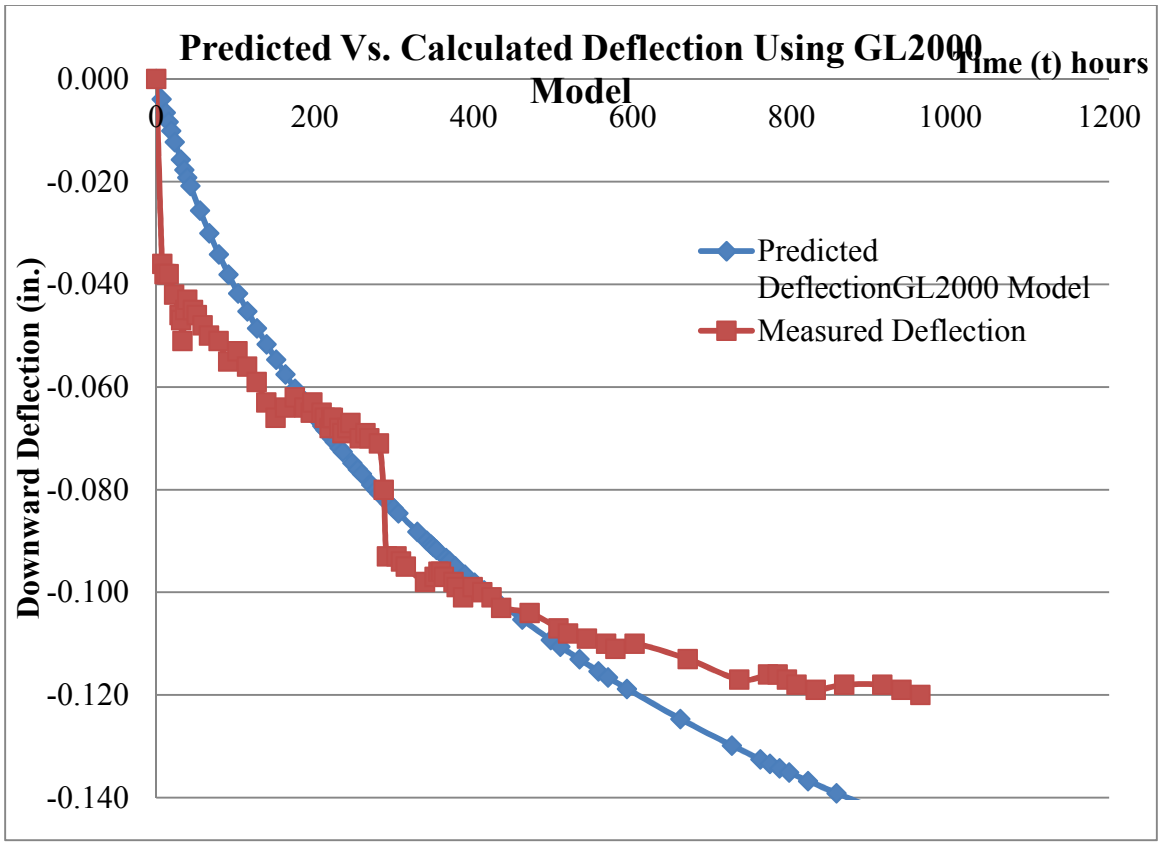

Figure 53 GL2000 model giving a good prediction for deflection for beam#2

4.7 Predicted Tensile Stress in Concrete Deck Slab:

Figure 54 shows the estimated tensile stresses using the four models. Figure 54 gives values for prototype beam# 1 while figure 55 gives values for beam# 2.

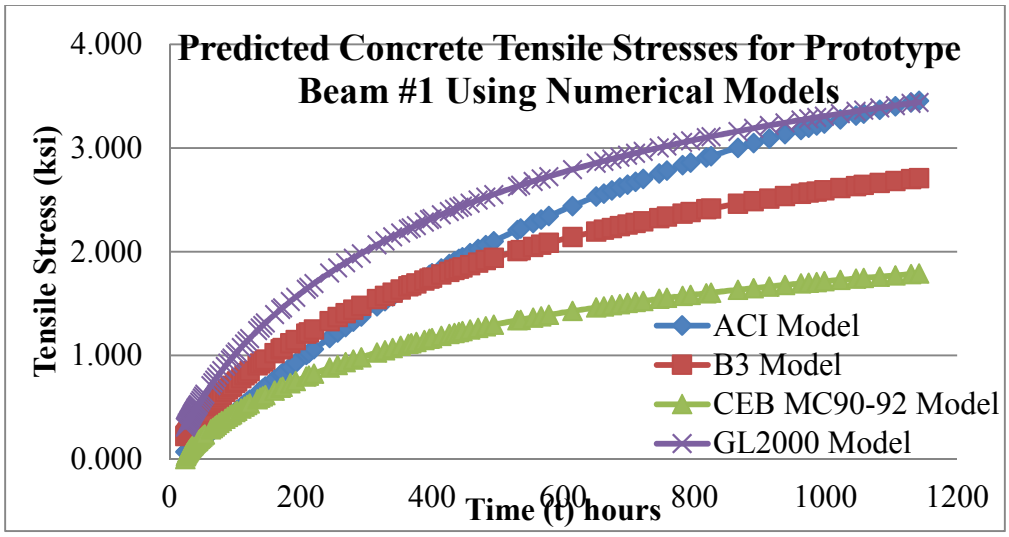

Figure 54 CEB model underestimates shrinkage strains and consecutively the tensile stress, GL2000 and B3 models tend to give a good prediction.

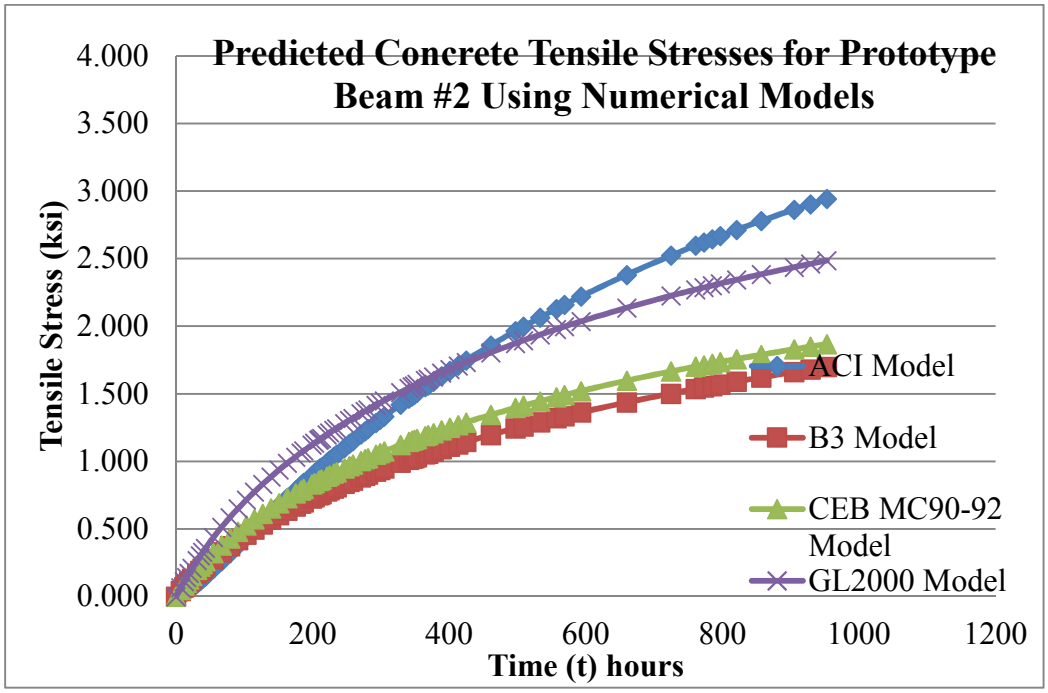

Figure 55 Predicted tensile stresses for prototype beam # 2 using the four numerical methods.

Figure 56 from field investigations, cracking occurs at regular patterns

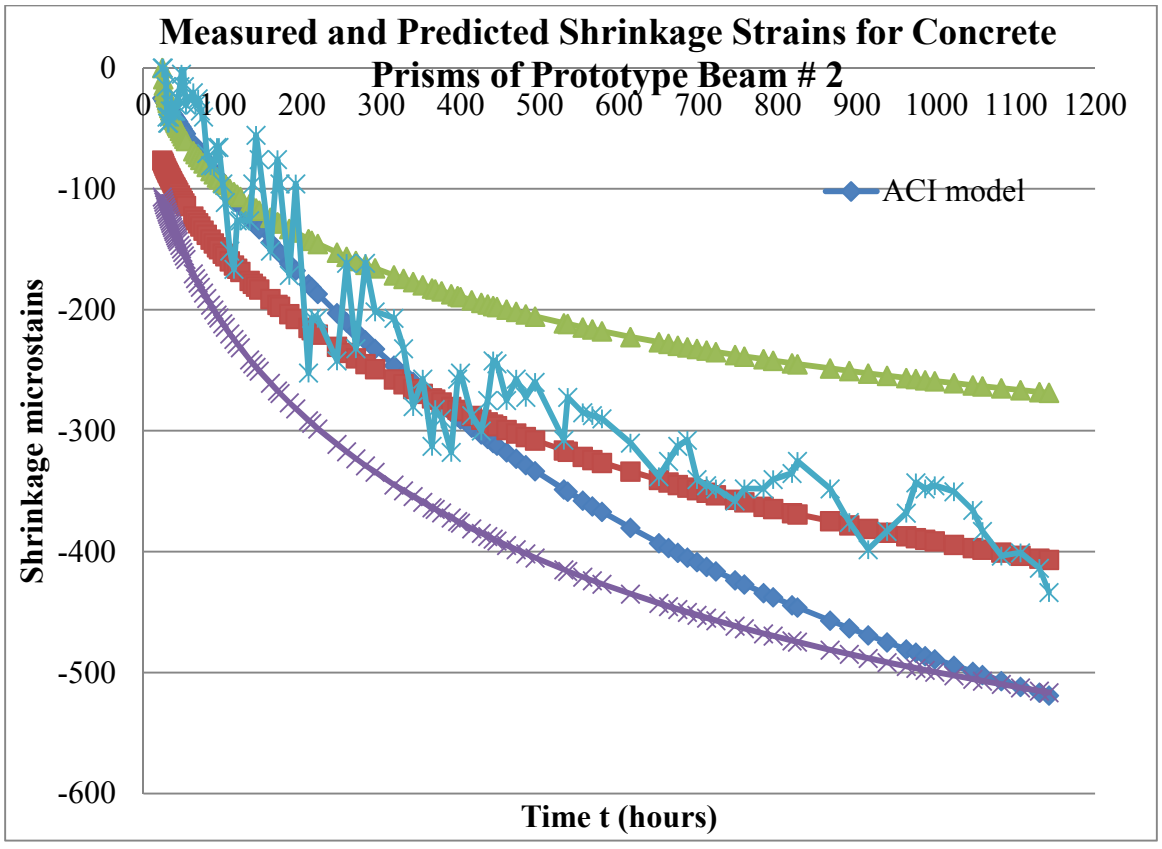

Figure 57 All shrinkage strain models compared together for beam # 1

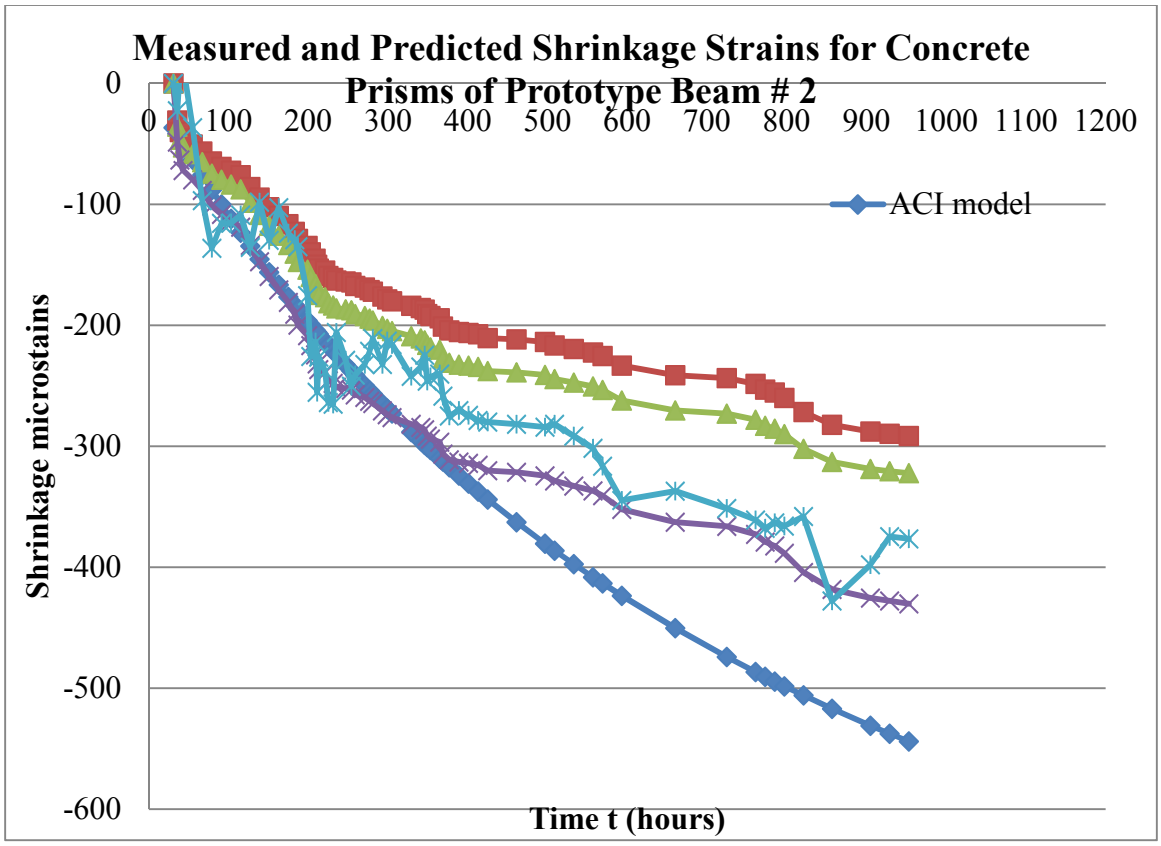

Figure 58 All shrinkage strain models compared together for beam # 2

CHAPTER V

DISCUSSION

From the laboratory testing, the concrete shrinkage of ODOT AA mixture is in the range of 500 microstrains. The shrinkage strains should continue to increase with time, though it is expected that the rate of increase will continuously decline. The mathematical models show that, at least theoretically, the shrinkage strains are sufficient to cause downwards deflections in the bridge decks made composite with steel beams. This is exhibited theoretically in the thesis and also experimentally from the results of the prototype beam tests.

However the theoretical model assumes elastic behavior for the concrete deck, which means the concrete deck is not cracked. However, I note from , the site visits, and as shown in Figure 56, that the concrete decks of the SH86 exhibited semi-regular crack patterns. This indicates that cracking is likely in real bridges..

Also, the Prototype beams demonstrated slab shrinkage matching the theoretical modeling to a great extent, although they were not cracked. This could be because of the fact that the change in temperature in the lab is very minimal and that the Prototypes were not subject to any type of loading. The concrete now is nearly a year old and has not yet cracked.

From laboratory testing for the tensile stress ASTM C496, the tensile stress was 300 psi at 3 days and nearly 600 psi at 28 days, from figure 25, the tensile strength almost takes 24 hours to develop most of it. Comparing that to the values obtained from theoretical models, we find that the tensile stress in the theoretical model can reach beyond 600 psi, which means the concrete slab can crack, which did not happen in the prototype beams. What is really important is not the fact if the concrete will crack or not, but the effect of the cracks on the curvatures due to shrinkage, in another words, will those cracks act as a relief for the restrained shrinkage taking place in concrete and said to be causing downwards deflection; this needs further research.

Models used in this research are all longer term for predicting shrinkage of concrete, assuming at least 7 days of moist curing, but the models can be easily modified to account for different conditions than the standard using correction factors. Models can be used for sand lightweight, normal weight and all lightweight concrete, also for any cement types and different curing conditions.

All the models mainly require basic information from the concrete mix, fresh concrete properties and hardened properties. Missing values can be assumed.

Basic information includes the age of concrete when moist curing ended, which is one day for our prototypes, curing method, relative humidity, concrete slump, air content and cement type.

The ACI model is the simplest one since it requires the least background knowledge and is also easy to adjust to match short term data.

From figures 36, 37, 38 and 39, ACI model shows to give better prediction at earlier ages, it tends to under-estimate shrinkage at higher ages. But still it is an easy way to predict shrinkage strains and deflections due to them. To get better results, a better estimate for the ultimate shrinkage strain can be considered from laboratory measurements, also accurate inputted data for mix proportions and concrete properties will help getting more accurate results out of this model.

The B3 model requires more inputs, like the shape of specimen, volume to surface ratio and water content. Also it models the Modulus of Elasticity for getting more accurate results. Comparing the tested values for elastic modulus of elasticity and estimated ones using figure 40, the tested and estimated elastic modulus matches really well at higher ages, at early ages the tested values are higher, which goes back to the fact that the elastic modulus is more dependent on the stiffness of the coarse aggregate – and less dependent on the actual strength of the concrete. For this reason, concrete typically will gain elastic modulus more rapidly at early ages than it gains strength.

Going back to the B3 model, the model matches the measured strain for the prototype beam# 1 but tends to over-estimate the shrinkage strains for beam#2. I attribute that to the sensitivity of this model to water content as stated in the ACI 209.2R-08 report. Since the beam# 2 has higher slump than beam# 1(9 in. compared to 4.5 in.).

The CEB model has this advantage of sub-dividing the shrinkage into autogenous and drying shrinkage, adding both together gives the total shrinkage. This showed that the autogenous shrinkage is time dependant while the drying shrinkage depends more on the concrete moisture and the relative humidity. The autogenous shrinkage showed to

develop really fast and then remains almost constant over time. Also it had a minimal contribution to the total shrinkage which makes it acceptable to ignore it and just count for the drying shrinkage. The disadvantage of the model that it clearly underestimated the shrinkage, the predicted values for the shrinkage strains were lower by a considerable amount. Also it is not easy to adjust for the use at early ages.

The last model used was the GL2000 which conforms with the ACI guidelines. Data needed to use this model is minimal, also it models the concrete compressive strength.

The model worked very well for prototype beam#2 but it overestimated the shrinkage strains for beam#1, model is sensitive to inputted concrete compressive strength.

The steel strains showed to be consistent with the change in temperature, so shrinkage in concrete slabs is assumed not to contribute to the strain happening in steel girders.

The compressive strains in the prisms were increasing at earlier ages then started to decelerate, median values of 450 microstrains were reached in 60 days.

Allowing partial slip between the concrete slab and steel girder will reduce the deflection induce due to slab shrinkage, reason is that the shrinkage will not be fully restrained, so the restraining force acting on the cross section will be less, which will reduce bending strains and thus curvature and deflection. This may be a good approach to counter-act the effect of concrete shrinkage on supporting beam although it will decrease the cross section capacity which is not good. In field less number of shear connectors will be required with re-organizing them to ensure some slip to happen, but again I will not recommend this.

CHAPTER VI

CONCLUSIONS AND RECOMMENDATION

6.1 Conclusions

Laboratory testing indicates that strains associated with volume change in concrete, including both temperature and drying shrinkage are large enough to be one possible cause for adverse deflections in steel girder bridges. Adverse deflections here mean unwanted deflections that may cause adverse ride quality or poor ride quality.

Furthermore, the analytical numerical models for predicting shrinkage strains and deflections in steel girder affirms that volume changes in concrete can cause the bridges to deflect downward, the models matched the strains and deflections measured in the laboratory prototype and concrete prisms associated to them. According to this it is likely that volume changes in concrete decks can be a reason for the problems related to the ride quality of the bridges. Having the models matching the measured strains and deflections means that the beams are in full composite action since it was assumed to have a full bond between the slab and the girder in the theoretical mechanics employed.

If cracks were to happen the effect of drying shrinkage can be mitigated but this cannot be said without further research.

The theoretical models used also don't account for cracking in the bridge decks, the prototypes demonstrates consistent shrinkage strains and deflections value with the numerical models noting that they did not crack too, which makes the model valid to compare to the prototypes.

From the results an allowance for deflections due to shrinkage of concrete deck slabs can be allowed or otherwise an approximate value like span/1500 can be used as a quick calculation for in service structures, the value of span/750 shown in the literature review is found to be high.

From the models used, the ACI model was found to be the easiest one with the minimal required input data required and less sensitivity to input change, so I highly recommend using it for predicting shrinkage strains and deflections in concrete.

If more accurate results are needed and more data are available in hand I would recommend using the B3 model for it has the advantage of developing time dependent elastic modulus to give better prediction for shrinkage strains and deflections than other models.

Although site investigations showed that cracking happens at semi-regular intervals, models can be used assuming elastic behavior, cracking as discussed earlier may act as a relief for the restraining action of shrinkage strains on composite beam, but this needs further research.

6.2 Recommendations

- Further research on the effect of cracking on the curvature due to shrinkage in composite beams.
- Limiting shrinkage strains is recommended to engineers as it is easy to consider using time dependent models, limitation can be done by using high quality aggregates, using multiple coarse aggregate sizes and limiting the cement content.
- Using pre-cambered steel girders when possible.

REFERENCES

ACI 209.2R-08. "Prediction of Creep, Shrinkage, and Temperature Effects in Concrete Structures (ACI 209R-92)". *American Concrete Institute* , 47.

ACI Committee 209. (2008). Guide for Modeling and Calculating Shrinkage and Creep in Hardened Concrete. *American Concrete Institute* .

ACI Committee 209. (1982). Prediction of creep, shrinkage and temperature effects in concrete structures. *ACI Special Publication* , 193-300.

ACI Committee 209. (1982). Prediction of creep, shrinkage and temperature effects in concrete structures. *ACI Special Publication* , 193-300.

ACI Committee 318. (1989). *Building code requirements for reinforced concrete (ACI 318-89).* Detroit.

Alexander, S. (2003). How Concrete Shrinkage Affects Composite Steel Beams. *New Steel Construction* .

Amadio, C., & Fragiacomo, M. (1997). Simplified Approach To Evaluate Creep AND sHRINKAGE eFFECTS in Steel-Concrete Composite Beams. *Journal of Structural Engineering* .

Bažant, Z. P., & Baweja, S. (1995,2000). Creep and Shrinkage Prediction Model for Analysis and Design of Concrete Structures—Model B3. *Materials and Structures , 28*, 357-365, 415-430, 488-495.

Bazant, Z., & Panula, L. (1978). Practical prediction of time-dependent deformation of concrete, Part 1. *Matériaux et Construction , 11* (5), 317-328.

béton, F. i. (1999). *Structural Concrete: Textbook on Behaviour, Design and Performance: Updated Knowledge of the CEB-FIP Model Code 1990.* FIB-Féd. Int. du Béton.

Birkeland, H. W. (1960). Differential Shrinkage in Composite Beams. *ACI , 56* (5), 1123-1136.

Branson, D., & Christiason, M. (1971). Time Dependent Concrete Properties Related To Design-Strength and Elastic Properties, Creep, and Shrinkage. *ACI Special Publication , 27*, 257-278.

CEB. (1991). "Evaluation of The Time Dependent Properties of Concrete,". *Bulletin d'Information, Comité European du Beton/Federation Internationale de la Precontrainte* , 201.

CEB. (1993). “CEB-FIP Model Code 1990,”. *CEB Bulletin D'Information* , 33-41.

CEB. (1993). “Structural Concrete—Textbook on Behaviour, Design and Performance. Updated Knowledge of the CEB/FIP Model Code 1990,”. *fib Bulletin 2 , 2*, 37-52.

CEB. (1999). “Structural Concrete—Textbook on Behaviour, Design and Performance. Updated Knowledge of the CEB/FIP Model Code 1990,”. *fib Bulletin 2 , 2*, 37-52.

Eguchi, K., & Teranishi, K. i. (2005). Prediction equation of drying shrinkage of concrete based on composite model. *Cement and Concrete Research* , 483-493.

Ferguson, P. M. (1958). Warping of Reinforced Concrete Due To Shrinkage. *ACI Journal , 30*, 1393-1398.

Gardner, N. J., & Lockman, M. J. (2001). Design Provisions for Drying Shrinkage and Creep of Normal Strength Concrete. *ACI Materials Journal , 98* (2), pp. 159-167.

J. C. (2001). Proceedings of symposium committee for the time-dependent deformation due to creep and shrinkage of the concrete structures. *JCI* , 101-121.

Kwak, H.-G., Seo, Y.-J., & Jung, C.-M. (2000). Effects of Slab Casting Sequences and the Drying Shrinkage of Concrete Slabs on The Short-term and Long-term Behavior of Composite Steel Box Girder Bridges. Part 1. *Engineering Structures* (23), 1453-1466.

Muller, H. S., & Hilsdorf, H. K. (1990). General Task Group 9. *CEB Comité Euro-International du Béton* , 201.

Russell, B. a. (1993). "Static and Fatigue Behavior of Pretensioned Composite Bridge Girders Made with High Strength Concrete". *PCI Journal , 38* (3), 116-128.

Russell, B. W. (1992).

Silfwerbrand, J. (1997). Stresses and Strains in Composite Concrete Beams Subjected to Differential Shrinkage. *ACI structural journal , 94*, 347-353.

Tonias, D. E. (1995). *Bridge Engineering.* New York: McGraw-Hill.

VITA

Ibrahim Abdelmeguid

Candidate for the Degree of

Master of Science

Thesis: SHRINKAGE INDUCED DEFORMATIONS IN COMPOSITE STEEL AND CONCRETE BRIDGES

Major Field: Civil/Structural Engineering

Biographical:

Education:

Completed the requirements for the Master of Science in Civil/Structural Engineering at Oklahoma State University, Stillwater, Oklahoma in May, 2015.

Completed the requirements for the Bachelor of Science in Civil Engineering at Cairo University, Giza, Egypt in 2011.

Experience: Structural/Bridge Engineer- Euro Consult, Cairo, Egypt.